EFFECT OF MODIFYING BRACE SLENDERNESS IN CONCENTRICALLY BRACED FRAMES

by

Timothy R. Eckert, P.E.

B.S. in Civil Engineering, West Virginia University, 2002

Submitted to the Graduate Faculty of

the Swanson School of Engineering in partial fulfillment

of the requirements for the degree of

Master of Science

University of Pittsburgh

2009

UNIVERSITY OF PITTSBURGH

SWANSON SCHOOL OF ENGINEERING

This thesis was presented

by

Timothy R. Eckert, P.E.

It was defended on

November 25, 2009

and approved by

Dr. John C. Brigham, Assistant Professor, Civil and Environmental Engineering

Dr. Piervincenzo Rizzo, Assistant Professor, Civil and Environmental Engineering

Thesis Advisor:

Dr. Kent A. Harries, Associate Professor, Civil and Environmental Engineering

EFFECT OF MODIFYING BRACE SLENDERNESS IN CONCENTRICALLY BRACED FRAMES

Timothy R. Eckert, M.S.

University of Pittsburgh, 2009

Steel moment-resisting frames are susceptible to large lateral displacements during severe earthquake ground motions leading engineers to turn to stiffer concentrically braced frames (CBF) as a way to resist earthquake loads. Braced framed systems are efficient because the lateral loads are resisted primarily by brace axial loads with little or no bending in the members. Brace behavior, however, is typically controlled by undesirable member buckling behavior. As a result, during cyclic loading, the brace hysteretic behavior is unsymmetric and there is deterioration of the building lateral load behavior. Buckling restrained braces (BRB) and partially buckling restrained braces (PBRB) have been proposed as alternatives to conventional brace design. Both use the steel section more effectively than conventional frames: BRBs achieve stable, symmetric hysteretic behavior by accommodating ductile compression yielding and thus can achieve the full theoretical capacity of the brace in both tension and compression. PBRBs, while not as efficient as BRBs, are ideal for the retrofit of existing braces since they can be built *in situ* with little impact on the surrounding structure. Additionally, the brace capacity is not affected, thus there is no need to retrofit the connections or subsequent elements of the force resisting system.

The objective of this thesis is to assess the potential design space of PBRBs. A series of analyses of a six story CBFs is conducted. The braces are provided with a range of hysteretic behaviors varying from that of a ‘slender’ brace to that of a BRB. Between these extremes, ‘intermediate’ and ‘stocky’ brace behavior represents the spectra of potential PBRB behavior. It is demonstrated that structural behavior is improved as the braces progressed from slender to stocky to BRB. The incremental improvement is most significant as one improves upon slender behavior and becomes less pronounced as the brace slenderness is reduced. This result is encouraging for the use of PBRBs as a retrofit measure for slender braces.

TABLE OF CONTENTS

LIST OF TABLES

LIST OF FIGURES

ACKNOWLEDGEMENTS

I would like to first thank my advisor and committee chair, Dr. Kent A. Harries, for his support and encouragement throughout the development of my thesis. I am fortunate for his time, expertise, and guidance.

I would also like to thank Dr. John C. Brigham and Dr. Piervincenzo Rizzo for serving on the committee and for giving me guidance and constructive criticism.

I would like to thank my fiancé, Jenny Kirkpatrick, for her support and patience throughout the course of this project.

Finally, I would like to give my unending appreciation to my parents, Bill and Susan Eckert for their unending support.

1.0 INTRODUCTION

1.1 BRACED FRAMES AS SEISMIC SYSTEMS

Steel moment-resisting frames (MRF) are susceptible to large lateral displacements during severe earthquake ground motions. In particular, special consideration to a) limit damage to nonstructural elements; b) address P-Δ effects; and c) mitigate brittle fracture of beam column elements are necessary when using MRFs in moderate and severe seismic zones. Often engineers turn to stiffer concentrically braced frames (CBF) as a way to resist earthquake loads. A common form of ordinary concentrically braced frame (OCBF) engages two-story X-bracing in which the centerlines of members form a truss system to resist lateral loads from earthquake and wind forces. The two-story X-brace typically spans two bays horizontally resulting in an architecturally acceptable solution in which each braced panel has only a single diagonal element (this better accommodates penetrations through the panel such as doors and windows). The two story braces are laterally braced at their mid length where they cross a floor diaphragm (see Figure 4.1). The length of such braces often results in the use of relatively large rolled shapes to resist large compression forces over their long length.

Braced framed systems are efficient because the lateral loads are resisted primarily by brace axial loads with little or no bending in the members. Brace behavior, however, is typically controlled by undesireable member buckling behavior. As a result, during cyclic loading, the

brace hysteretic behavior is unsymmetric in compression and tension and there is deterioration of the building lateral load behavior. Design simplifications often result in braces selected for some stories being stronger than required and others being closer to the target demand values. This variation in story capacity ratio, together with strength loss when some braces buckle, can result in earthquake damage being concentrated in a few stories. Such “soft-story” damage concentration puts greater stress on conventional braces and their connections. Additionally, lateral buckling of the braces may cause damage to other structural elements. Observation of damage that occurred during the 1989 Loma Prieta and 1994 Northridge earthquakes, particularly with regard to ultimate deformation of this type of frame system, resulted in renewed research efforts whose objectives were to improve braced frame behavior. During the last 20 years, increasing research on the ductility and energy dissipation of seismic-resistant structural systems has led to the development of special concentrically braced frame (SCBF) systems (Goel 1992 and Bruneau et al. 1998).

SCBF are intended to exhibit improved post-buckling capacity over OCBF. In an SCBF, the braces still buckle in compression but are designed to maintain a greater post-buckling capacity and thus continue to contribute to overall frame capacity. Additional special detailing of the connections that prevent local connection buckling failures and member failures even when there is overall buckling of the compression brace are also required in SCBFs. The required brace and connection detailing can be quite restrictive, resulting in braces fabricated from large rolled shapes.

Braced frame members are sized based on criteria such as: sufficient stiffness to satisfy code drift requirements and adequate member strength to resist both compressive and tensile axial forces. During earthquakes, the brace members undergo significant inelastic deformations

into the post buckling range and repeated tension and compression cycles. The SCBF ductility comes from axial inelasticity of the braces in tension and compression. Compression buckling, however, results in degradation of the brace stiffness and strength. Eventual plastic hinge formation can lead to brace fracture. Buckling of the braces, therefore limits the performance of the CBF system. Finally, the unsymmetric behavior between the tension and compression hysteretic behaviors leads to undesirable system response. Such observations have led to the development of buckling restrained braces which aim to mitigate the brace degradation resulting from compressive buckling.

1.2 BUCKLING RESTRAINED BRACES

Buckling Restrained Brace Frames (BRB) are a relatively new development for CBFs (Sabelli and Lopez, 2004). BRBs are comprised of a steel core that resists the axial brace stresses and a steel-encased concrete sleeve which provides buckling restraint to the brace. The sleeve is intentionally debonded from the internal brace core so as not to contribute to axial capacity. An example of BRB geometry is shown in Figure 1.1. BRBs use the steel section more effectively than conventional frames such as OCBF or SCBF, which depend on brace buckling for ductility. BRBs achieve stable, symmetric hysteretic behavior by accommodating ductile compression yielding and thus can achieve the full theoretical capacity of the brace in both tension and compression.

1.3 PARTIALLY BUCKLING RESTRAINED BRACES

Buckling restrained braces are proven systems that effectively stabilize brace members. However, these systems may not always be ideal especially in retrofitted structures because they are expensive, difficult to install, may result in different load distributions than originally intended, and they may also be overdesigned for structures in low to moderate seismic regions. Abraham and Harries (2007) introduced the concept of partially buckling restrained braces (PBRB) whose behavior would lie between that of a BRB and a conventional brace. In a PBRB, fiber reinforced polymer (FRP) composite materials are applied to the steel brace in an attempt to enhance the member's buckling capacity and hysteretic behavior. The FRP material is elastic to failure and thus is able to provide a 'bracing' force to a steel plate that has achieved plasticity. Conceptually, the FRP is used to constrain the plastic flow of the steel. Thus, the approach has been shown to be effective in cases of mitigating local buckling of slender elements but is less effective at mitigating the global elastic buckling behavior prevalent in long steel braces (Harries et al. 2009). Nonetheless, in even relatively long braces that buckle elastically, the presence of the FRP was noted to mitigate the inelastic 'kink' behavior that follows compression buckling. Thus Harries et al. proposed that the hysteretic behavior of a steel brace may be improved by mitigating local buckling and/or kink behavior. Figure 1.2 provides a schematic representation of the axial behavior of a steel brace and that which may be affected by a PBRB. This figure will be described in greater depth in Chapter 2.

PBRBs are ideal for the retrofit of existing braces since they can be built *in situ* with little impact on the surrounding structure. Additionally, the brace capacity is not affected, thus there is no need to retrofit the connections or subsequent elements of the force resisting system.

1.4 OBJECTIVE

The objective of this thesis is to assess the potential design space of PBRBs. A series of analyses of a six story CBFs is conducted. The braces are provided with a range of hysteretic behaviors varying from that of a 'slender' brace to that of a BRB. Between these extremes, 'intermediate' and 'stocky' brace behavior represents the spectra of potential PBRB behavior. The fundamental question addressed is: *When retrofitting a braced frame, is it always necessary to improve brace behavior to that of a BRB or, under some performance objectives is it adequate to provide something less: a PBRB?* Similarly: *Are BRBs necessary in regions of low or moderate seismicity? Are there applications where a slender, intermediate, or stocky brace will achieve the desired performance objectives?*

Cost comparisons are beyond of scope of this project, however in general, the cost of a brace is proportional to its axial capacity (cross sectional area) and degree of buckling restraint (confinement) provided. Thus, while a BRB may be an excellent system in terms of performance, this comes at a high cost.

1.5 OUTLINE OF THESIS

This work was separated into two phases: First, analytical studies of modeling behavior of slender, intermediate, stocky, and buckling restrained braces are presented. The Remennikov and Walpole (1997) brace hysteretic model will be validated by brace behavior reported by others in order to gain an understanding and confidence in modeling this relatively complex hysteretic behavior (Figure 1.2). This task is reported in Chapter 3. Second, the brace behavior

validated in the first task will be applied to the model of a six-story split level X-braced frame. The same frame will be modeled as having slender, intermediate, stocky and buckling restrained braces. The structural behavior will be compared to assess the effects of changing brace parameters. This task is reported in Chapter 4. Both tasks use the nonlinear frame analysis program RUAUMOKO (Carr 2002) and are complemented by a literature review presented in Chapter 2.

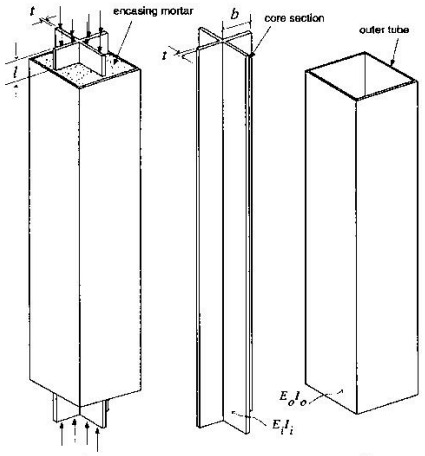

a) Schematic of unbonded buckling-restrained brace and its components (Black et al. 2004)

b) Unbonded BRB awaiting testing at E-Defense (photos: Harries)

Figure 1.1 Buckling restrained braces (BRB).

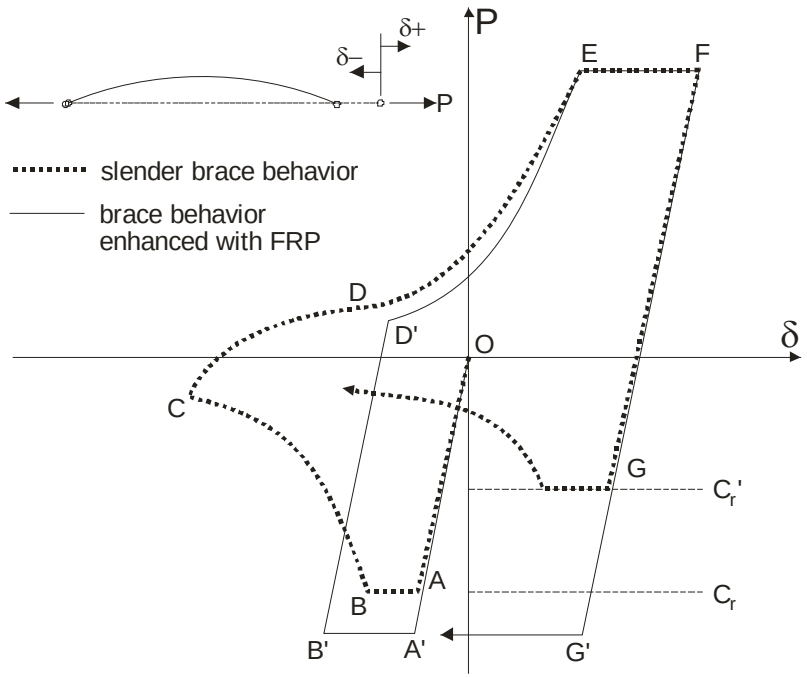

Figure 1.2 Sample brace hysteresis modified to reflect reduced "kinking" behavior. (Harries et al. 2009)

2.0 LITERATURE REVIEW

This chapter presents background information on hysteretic brace behavior. Representative research on experimental brace behavior is presented. This experimental brace behavior is compared to the analytical behavior described by Remennikov and Walpole (1997) which will be used in the present study.

2.1 BRACE BEHAVIOR

For the sake of this work, a brace is a structural element carrying only axial loads which is subjected to stress reversals. The prototype considered throughout the discussion is a brace element in the lateral force resisting system of a concentrically braced frame (CBF) subject to seismic loading. The complete brace behavior under repeated stress reversals is referred to as its hysteretic behavior. The brace behavior is described by the hysteretic response of applied axial load (P) plotted against resulting axial deflection (δ). The area under the P-δ curve indicates the amount of hysteretic energy the member dissipates. Figure 2.1 illustrates the idealized hysteretic behavior of a typical bracing member (Bruneau et. al 1998). The axial load (P), axial displacement (δ), and lateral displacement at mid length (Δ) are utilized to describe this behavior. Tension forces are positive. Only flexural torsional buckling (FTB) is considered; i.e.: the brace

section is assumed to be compact and therefore not susceptible to flange or web local buckling (FLB or WLB).

Considering Figure 2.1: loading begins at the origin (point O) and the brace is compressed elastically. Flexural buckling (FTB) occurs at point A, and the brace deflects laterally in an elastic manner. FTB occurs at a critical buckling load, C_r, which may be determined from the Euler buckling equation accounting for brace slenderness and boundary conditions:

$$C_r = A_{brace}\,\sigma_{cr} = A_{brace}\,\frac{\pi^2 E}{(kL/r)^2} \qquad (Eq.\,2.1)$$

Where A_{brace} = sectional area of brace member;

E = elastic modulus of brace

k = effective length factor associated with boundary conditions

L = length of brace

r = radius of gyration of brace about buckling axis

At point B, a plastic hinge forms where the brace plastic moment capacity is exceeded by the moment induced by the now-eccentric load, PΔ. For a uniform brace this occurs at the mid length where the lateral displacement, and therefore moment is greatest. A further increase in axial displacement results in increased lateral displacement at the plastic hinge as the hinge rotates. The hinge region has no further stiffness and thus this rotation manifests itself as a ‘kink’ in the brace deflected shape. With continued axial displacement (points B to C), the brace capacity falls (effectively, the brace has a ‘negative stiffness’ as the hinge rotates). With unloading of compression forces, the still-elastic portions of the brace result in a reduction in the lateral deflections (points C to D) which exacerbates the ‘kink’ (which does not recover elastically). As the brace force reverses into tension (points D to E) the moments on the hinge are

reversed and the lateral deflection is recovered. However, the resistance of the 'kinked' hinge region is significantly less than the axial stiffness of the brace resulting in a region of very low stiffness between points D and E as the kink is straightened. Finally at point E, the tensile capacity of the brace is achieved and maintained (points E to F) although there is a residual lateral displacement at the kink (shown schematically on the right hand side of Figure 2.1). When the brace reloads in compression, the residual lateral displacement serves to reduce the compression buckling capacity of the brace (point G). The residual buckling capacity of the brace is defined as (AISC 2005b):

$$C_r' = \frac{C_r}{1+0.50\left|\frac{kL}{\pi r}\sqrt{\frac{0.5F_y}{E}}\right|} \qquad (Eq.\ 2.2)$$

Where F_y is the yield stress of the brace material and C_r is defined in Eq. 2.1

Braces are described as being 'slender' when their slenderness ratio, $\lambda = kL/r$, is greater than 120. Braces are 'stocky' for $\lambda < 50$ and 'intermediate' between these limits. Stocky braces are dominated by section yielding and local flange or web buckling. Local buckling results in a loss of moment capacity at the plastic hinge location. Previous research (Bruneau et al. 1998) has shown that for stocky braces, the large section distortions initiated by local buckling of a flange will likely lead to global buckling. Intermediate braces experience global buckling at an apparent critical buckling stress that is reduced from the nominal yield value. Intermediate brace behavior is affected by the presence of residual fabrication stresses. Slender braces exhibit elastic FTB behavior where no portion of the cross section exhibits yield. Figures 2.2 and 2.3 contrast the behavior of stocky, intermediate and slender braces. All braces can reach their tensile capacity since buckling is not an issue in tension. In compression, however, stocky braces reach a higher buckling load (C_r) and exhibit a greater hysteresis (energy dissipated as measured by area under

the hysteresis curve) than intermediate and slender braces. Additionally, stocky braces exhibit less stiffness degradation upon reloading from tension to compression (region D in Figure 2.1). The behavior of intermediate and slender braces is said to be 'pinched' as the stress range from tension to compression at zero displacement becomes increasingly smaller. Additionally, slender braces exhibit greater degradation of compression strength and reloading stiffness with subsequent cycles (Figure 2.3a). Finally, due to the pronounced kinking, slender braces become susceptible to fracture in the hinge region due to low cycle fatigue; i.e.: fracture due to a small number of excursions to very high strains. Thus stocky braces are preferred in conditions of dynamic loading for their superior energy absorption and post-buckling performance. Bruneau and Lee (2005) demonstrated that energy dissipation capacities of intermediate or slender braces are similar and significantly less than that of stocky braces.

Black et al. (1980) studied the impacts of slenderness, end conditions, and different structural shapes on hysteretic brace behavior through experimental research. This research became the benchmark for understanding brace cyclic behavior. Black et al. considered slenderness ratios varying from 30 to 150 and structural shapes including double-channels, W-sections, double-angle sections, WT sections, and square tubes. Black et al. concluded that slenderness ratios have a greater impact on the hysteretic brace behavior than end conditions and/or structural shape. Furthermore, they concluded that maximum compressive loads deteriorated more with slender braces. End conditions were seen to affect behavior to a greater degree when inelastic deformations were present (stocky braces).

2.2 BUCKLING RESTRAINED BRACE BEHAVIOR

Buckling restrained braces (BRB) increase the compressive capacity of braces while not affecting the tensile capacity in order to produce a symmetric hysteretic response as is shown in Figure 2.4. They achieve this through the decoupling of the axial stress-resisting and flexural buckling-resisting aspects of the compression strength. Buckling restrained braces have predictable and ductile behavior and large plastic deformation capacity in both tension and compression; therefore large amounts of seismic energy can be absorbed by this type of brace. This is important because although the frame may sustain significant damage during an earthquake, it is expected to remain stable and the building must be capable of resisting gravity loads and of withstanding aftershocks without collapse. This behavior is achieved by allowing the core brace to deform longitudinally independent of the encasing system. The encasing system is intended to increase the radius of gyration to the point that FTB is mitigated and also restrain the brace section to mitigate FLB or WLB. This allows the brace to have large inelastic capacities, thereby 'protecting' the other elements of the structure from large inelastic demands. For this reason, interstory drifts are expected to be much lower for concentrically braced frames (CBF) having BRBs as compared to those with conventional braces – even if they are stocky braces. The advantage of BRBs is that the brace core, may now be designed for its full section capacity resulting in a more efficient use of material. In a BRB, the brace core is likely slender without considering the encasing system. Black et al. (2004) identified three possible buckling modes of failure during stability analysis of BRBs: a) global flexural buckling (FTB) of the entire brace; b) buckling of the inner core in higher modes; and c) plastic torsional buckling of the projection of the steel core outside of the confining tube in the connection region. Black et al.

showed that these modes may be mitigated and the brace core plastic capacity achieved in both tension and compression when good detailing is provided.

2.3 PARTIALLY BUCKLING RESTRAINED BRACE BEHAVIOR

Partially buckling restrained braces (PBRB) utilize fiber reinforced polymer (FRP) composite materials to provide local or global support to the brace member. While not as efficient as BRB, PBRB hysteretic behavior is characterized as falling between BRB and conventional brace behavior (Harries and Abraham, 2006). PBRB were specifically proposed as retrofit measures for slender braces to affect their behavior so that it 'moves up the spectra' to that of intermediate braces (and/or shifting intermediate brace behavior to that of stocky).

Harries and Abraham (2006) studied WT shapes to predict the hysteretic behavior of the PBRB. They demonstrated that the presence of FRP material on the slender web of the WT section considered inhibited the inelastic kinking behavior and ultimately may allow the section to resist a greater amount of cyclic loading. The theoretical effect of mitigating the kinking effect is illustrated in Figure 2.5. By mitigating the kinking:

1. The compression "plateau" A-B is elongated;
2. The residual compressive load C_r' may be increased;
3. The 'negative stiffness' region (B-C) is minimized or mitigated altogether;
4. The reloading tensile stiffness (C-D-E) is increased;
5. The rapid transition in stiffness during tension reloading (D-E) is less significant; and

6. The number of cycles to eventual fracture of the section due to low cycle fatigue is increased due to the reduced plastic deformation demand.

Each of these effects affect an increase in energy that may be dissipated by the brace as illustrated by a greater area contained under the hysteresis in Figure 2.5.

2.4 MODELING OF BRACE BEHAVIOR

Frame element models which are used to model the inelastic behavior of steel braces, can alternatively be classified as finite element, phenomenological, or physical theory models (Ikeda and Mahin, 1986). Finite element models are the most time consuming and computationally expensive. Phenomenological models are based on simplified hysteretic rules that are dependent on axial force and axial deformation only. Physical theory models are based on force, deformation and other factors that influence inelastic brace behavior. They consider such parameters as yield strength, modulus of elasticity, and geometric properties. The Ikeda (1986) model is a physical model consisting of a pin-ended bracing member with a plastic hinge forming at midspan. Braces with other end conditions may be modeled using the concept of effective length. The modeled hysteretic behavior involves the buckling of the element, local buckling effects, yielding of the material, and post-buckling deterioration of the axial capacity related to the Bauschinger effect. Figure 2.6 demonstrates the modeled hysteretic behavior which is broken up into four elastic regions (ES1, EL1, EL2 and ES2); two inelastic (plastic) regions (P1 and P2); an elastic buckling region (BU), and a tensile yield region (PY). The terms ‘elastic’

and ‘plastic’ in these descriptions refer to the state of the plastic hinge and the term ‘yield’ is related to the brace segments outside the hinge.

Remennikov and Walpole[1] (1997) developed an incremental mathematical model to implement the Ikeda (1986) physical model in a finite element routine. The R-W model has been programmed into the open source nonlinear dynamic analysis program RUAUMOKO (Carr 2002). The R-W hysteresis requires the input parameters described in Table 2-1

To gain an understanding of the R-W model and the interaction of parameters, the behavior of three prototype braces reported by Black et al. (1980) (hysteretic envelopes shown in Figure 2.2) were modeled using the R-W hysteresis as incorporated into RUAUMOKO. The results were validated against the experimental results reported by Black et al. This validation study of the R-W hysteresis model is presented in Chapter 3. Having gained an understanding of the R-W behavior, nonlinear dynamic modeling of prototype frame structures having different brace behaviors is presented in Chapter 4.

[1] For convenience, the Remennikov-Walpole model will be referred to as the R-W model in this work.

Table 2-1 R-W model parameters.

parameter (see Figure 2.6)	**RUAUMOKO input parameter**	**description** (Carr 2002)	**note**
I_{minor}	I_{minor}	minor axis moment of inertia	R-W assumes minor axis buckling; i.e.; $I_{major} > I_{minor}$
Z_{minor}	S_{minor}	minor axis plastic section modulus	
k	k	effective length factor	$L_{eff} = kL$
	α	strain hardening factor	accounts for post-yield strain hardening stiffness
	β	'beta' factor	mathematical factor affecting pinching behavior
	θ_0	initial out of straightness	not considered in this study but allows for initial imperfections in the brace to be considered; essentially increasing the moment on the hinge region
ES1	E1	effective modulus	
EL1	E2	effective modulus	
ES2	E3	effective modulus	
	E4	effective modulus	control parameter defining transition from ES2 to ES1 and EL1 to EL2
	N	strain hardening rule selection	strain hardening using α (N=0) or built in RUAUMOKO strain hardening rule (N = 1)
	SHAPE	cross section type	hinge behavior modified for flanged or closed (i.e.: box) cross section

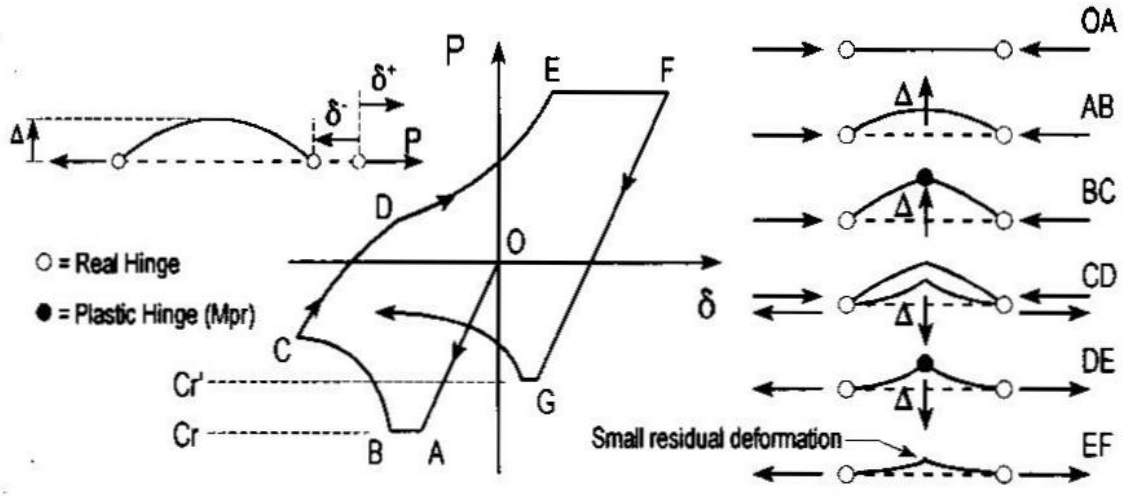

Figure 2.1 Sample hysteretic behavior of bracing member. (Bruneau et al. 1998)

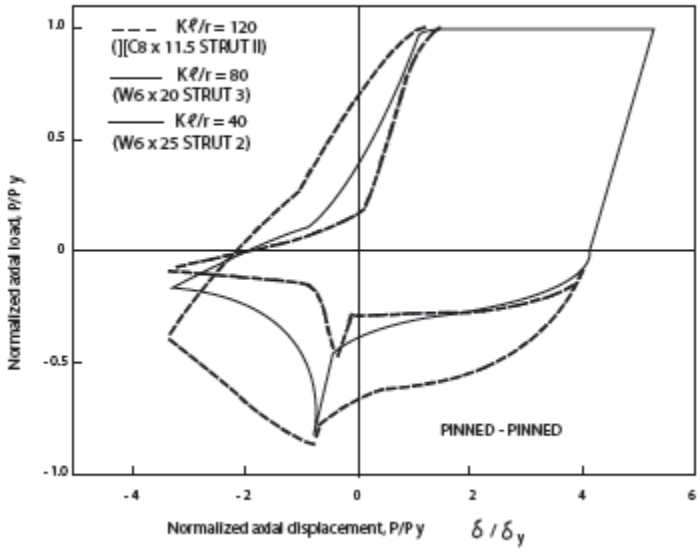

Figure 2.2 Normalized hysteresis envelopes. (Bruneau et al. 1998 from Black et al. 1980)

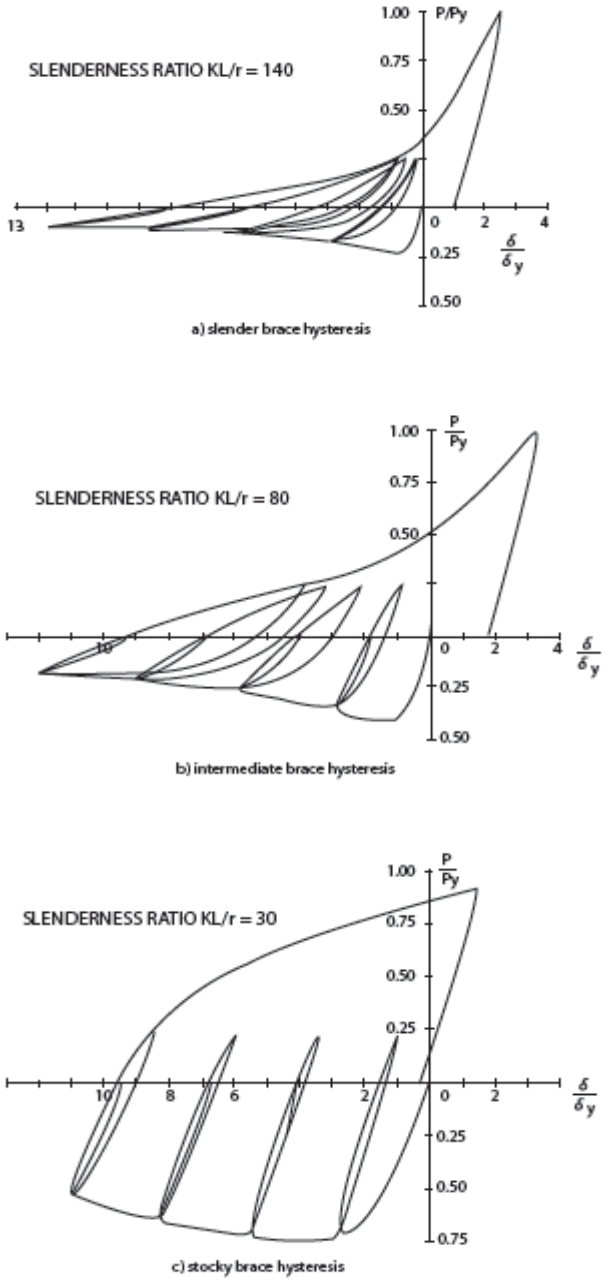

Figure 2.3 Sample hysteretic responses. (Bruneau et al. 1998 from Jain 1978)

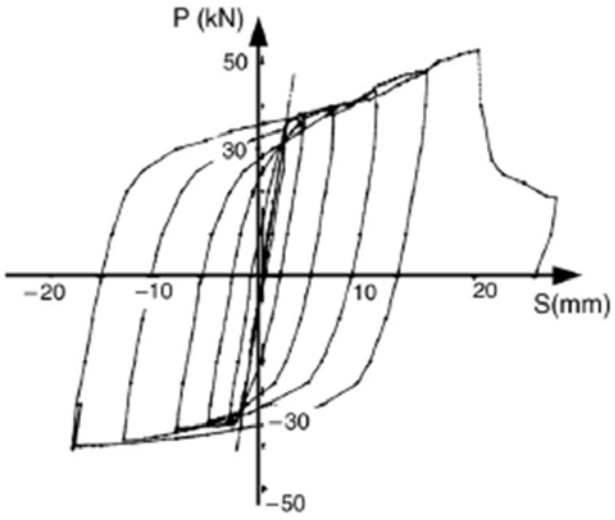

Figure 2.4 Hysteretic response of BRB. (Xie 2005 from Wakabayashi et al. 1973)

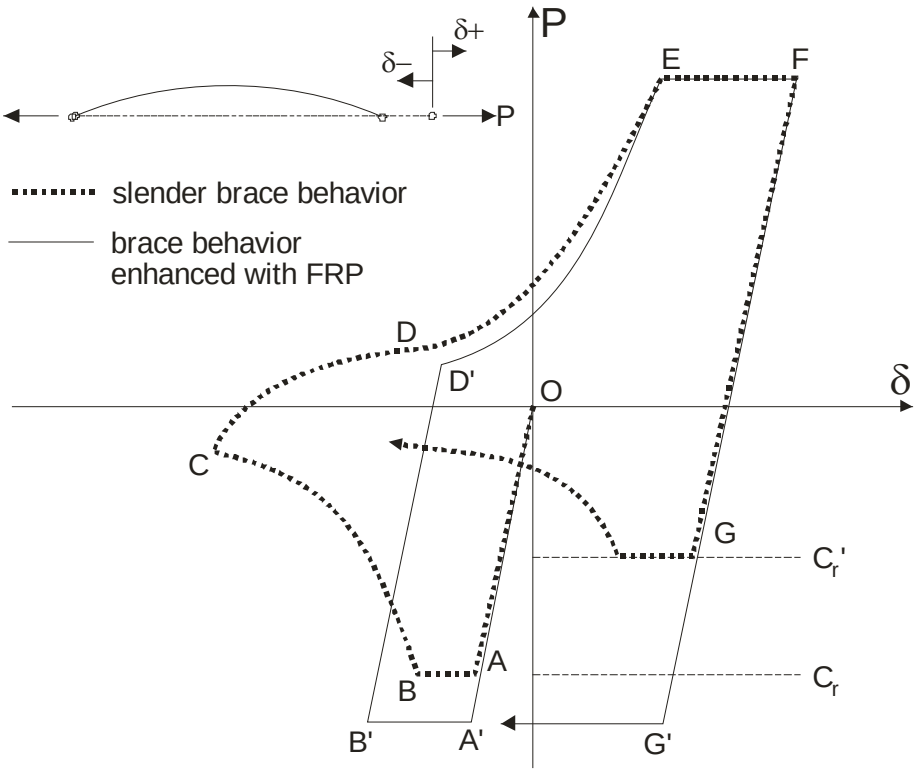

Figure 2.5 Sample brace hysteresis modified to reflect reduced "kinking" behavior. (Harries et al. 2009)

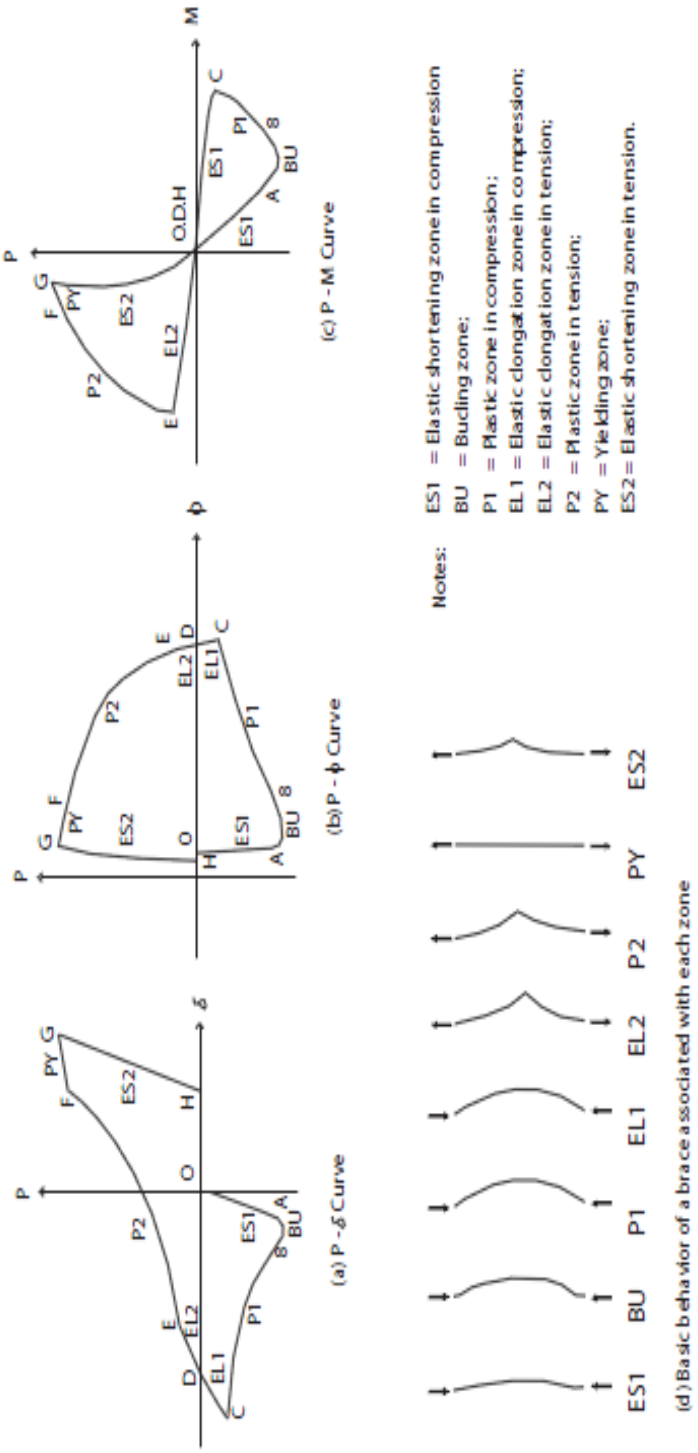

Figure 2.6 Brace load-deflection curve modeled by Remennikov and Walpole. (Carr 2002 from Ikeda and Mahin 1986)

3.0 MODELING BRACE HYSTERETIC BEHAVIOR

This work was exploratory in nature and relied on an iterative process to conclude that the desired brace behavior had been achieved. The objective of the brace modeling task described in this chapter was to gain an understanding of how the Remennikov-Walpole (R-W) hysteretic model behaved. A study, varying the R-W input parameters (Table 2-1) was conducted to investigate the effect of each parameter on the prototype hysteretic curves. Available experimental curves given in Chapter 2 were used to validate the brace behaviors obtained and to therefore gain confidence in the application of the complex R-W model behavior.

3.1 APPLICATION OF R-W MODEL IN RUAUMOKO

The nonlinear finite element analysis program RUAUMOKO[2] (Carr 2002) was used in this study. RUAUMOKO is an open-source, primarily frame element-based program intended for research applications involving the seismic analysis of building structures. One of the strengths of RUAUMOKO is that it incorporates a large number of hysteretic models developed for a variety of special applications. RUAUMOKO includes coding for the R-W model.

[2] Ruaumoko is the Maori deity responsible for earthquakes. RUAUMOKO was developed at the University of Canterbury, New Zealand.

The HYSTERES module of RUAUMOKO permits the rapid modeling of a single element subjected to a standard experimental hysteresis. The module is intended for the validation and tuning of hysteretic models against experimental results. HYSTERES uses a defined displacement history and computes the associated hysteresis for a given member having specified stiffness, yield strength and post-yield behavior. This program may be used to see how a particular hysteresis model works but may also be used to determine the best choice of parameters to obtain the most suitable hysteresis loop for use in a RUAUMOKO analysis (Carr 2002). HYSTERES was used in the present study to gain an understanding of the performance of the R-W model. The model was validated against the experimental stocky, intermediate and slender brace hystereses reported by Black at al. (1980) whose envelopes are shown in Figure 2.2.

A single beam-column element is modeled; the selection of the R-W hysteretic model automatically results in only the consideration of axial behavior of this element (i.e.: rotational degrees of freedom at beam ends are released). The element was subjected to a displacement history similar to that used in the experimental program against which the model is being compared. The HYSTERES displacement history used consists of single progressively increasing displacement cycles as shown in Figure 3.1.

Apart from the brace section properties, an iterative approach involving selecting brace parameters and validating the behavior against that reported by Black et al. (1980) was carried out. The resulting parameters used are given in Table 3-1. The resulting hysteretic behaviors are shown in Figure 3.2.

By using this iterative approach, one can see how each of the variables affects the hysteretic curves (Figure 3.2). The effective length was changed to obtain the desired brace type

that was studied. The β factor is the parameter that affects the pinching behavior. β varied from 1.2 to 1.4 as the behavior varied from slender to stocky. The effective modulus controls the transitions from ES1 to ES2 and EL1 to EL2 as described in Chapter 2. During the validation study, these variables remained the same for all braces as they were not found to have a significant effect on behavior. The plastic zone in tension (P2 in Figure 2.6) transforms from a 'flat' slope for a slender brace to a 'steep' slope for a stocky brace. The plastic zone in compression (P1) goes from a 'steep' slope for a slender brace to a 'flat' slope for a stocky brace. These characteristics are most significant in modeling brace behavior. The results from the validation study shown in Figure 3.2 demonstrate a close representation of the experimental results shown in Figures 2.2 and 2.3. Significantly, the post-yield behavior and residual buckling capacity described by Eq. 2.2 is captured very well.

3.1.1 Brace Capacity

HYSTERES requires initial brace tension and compression capacities. These were determined in accordance with AISC (2005) requirements without accounting for material reduction factors. The axial tension capacity of the braces is defined as:

$$T_{CAP} = A_g F_y \qquad (Eq. 3.1)$$

Where A_g is the gross cross section area of the brace and F_y is the yield strength of the brace taken as 36 ksi in this study.

The axial compression capacity of the brace is defined as:

$$C_{CAP} = F_{CR} A_g \qquad (Eq. 3.2)$$

Where the critical inelastic buckling stress, F_{cr}, of the brace is given as:

$$F_{CR} = \left(0.658^{\frac{F_y}{F_e}}\right) F_y \qquad (Eq. 3.3)$$

The Euler buckling capacity, F_e, is:

$$F_e = \frac{\pi^2 E}{\left(\frac{KL}{r}\right)^2} \qquad (Eq.\ 3.4)$$

Where KL/r is the slenderness ratio and E is Young's modulus of the brace taken as 29000 ksi in this study.

3.2 BRB MODELING

For completeness and eventual comparison, BRB behavior was also modeled and validated using HYSTERES. Due to its simpler behavior, the BRB prototype is modeled with the bi-linear hysteresis model shown in Figure 3.3. The modeled BRB behavior is shown in Figure 3.4 and compares well with the behavior against which it was validated shown in Figure 2.4. (Wakabayashi et al. 1973).

3.3 SUMMARY OF BRACE MODELING

The results presented in this chapter demonstrate the applicability of using the R-W hysteresis model to model the behavior of braces having varying slenderness. The 'lessons learned' in conducting this validation study and the resulting understanding of R-W input parameters are adopted in the braced frame study presented in Chapter 4.

Table 3-1- R-W input values used for validation study

RUAUMOKO input parameter	**description** (Carr 2002)	**Slender**	**Intermediate**	**Stocky**
I_{minor} (in^4)	minor axis moment of inertia	2.62	13.3	17.1
S_{minor} (in^3)	minor axis plastic section modulus	1.55	4.41	5.61
k	effective length factor	1.0	1.6	0.8
α	strain hardening factor	1.0	1.0	1.0
β	'beta' factor	1.2	1.3	1.4
θ_0	initial out of straightness	0.0	0.0	0.0
E1	effective modulus	1.0	1.0	1.0
E2	effective modulus	1.0	1.0	1.0
E3	effective modulus	1.0	1.0	1.0
E4	effective modulus	1.6	1.6	1.6
N	strain hardening rule selection	0	0	0
SHAPE	cross section type	1	1	1

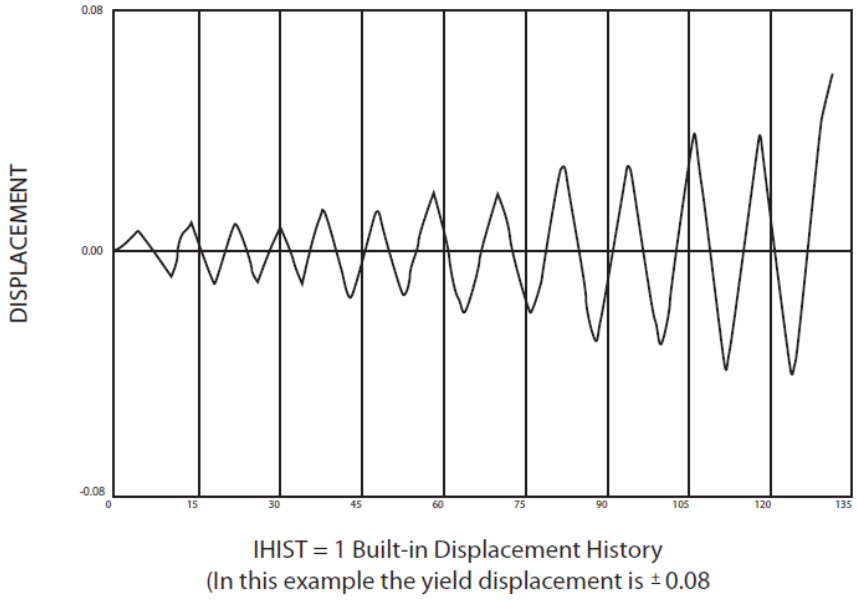

Figure 3.1 HYSTERES displacement history used to model brace members. (Carr 2002)

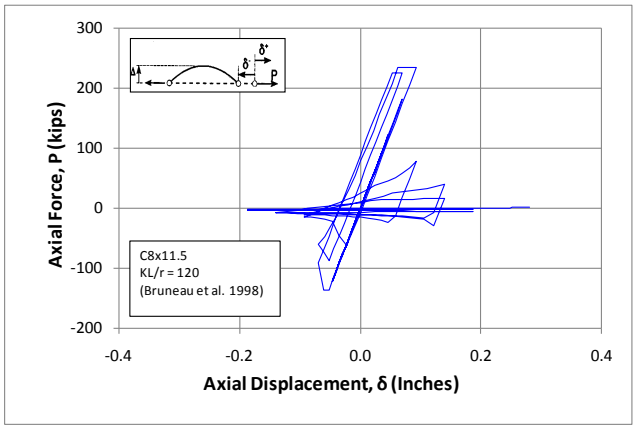

a) slender brace hysteresis

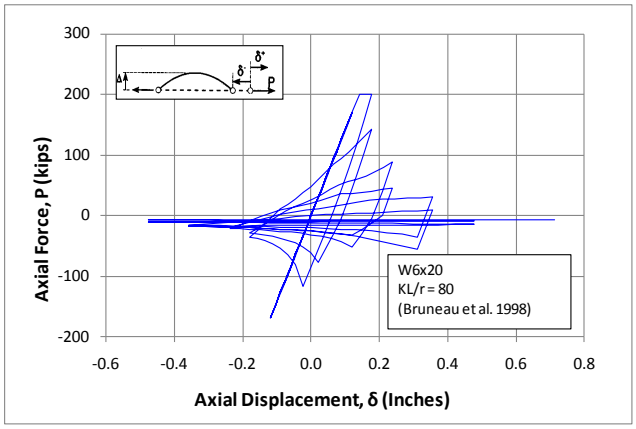

b) intermediate brace hysteresis

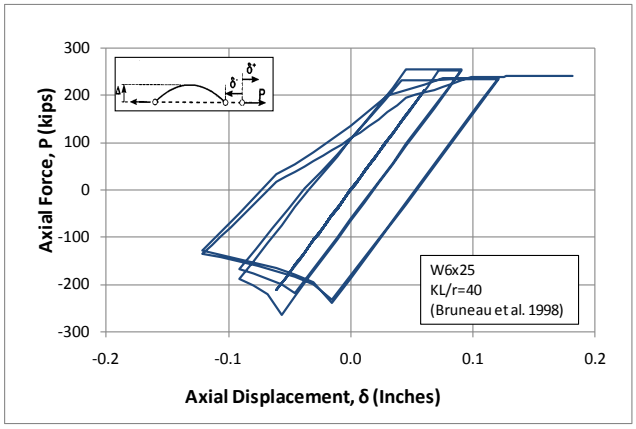

c) stocky brace hysteresis

Figure 3.2 HYSTERES-modeled hysteretic brace behaviors modeled using R-W model

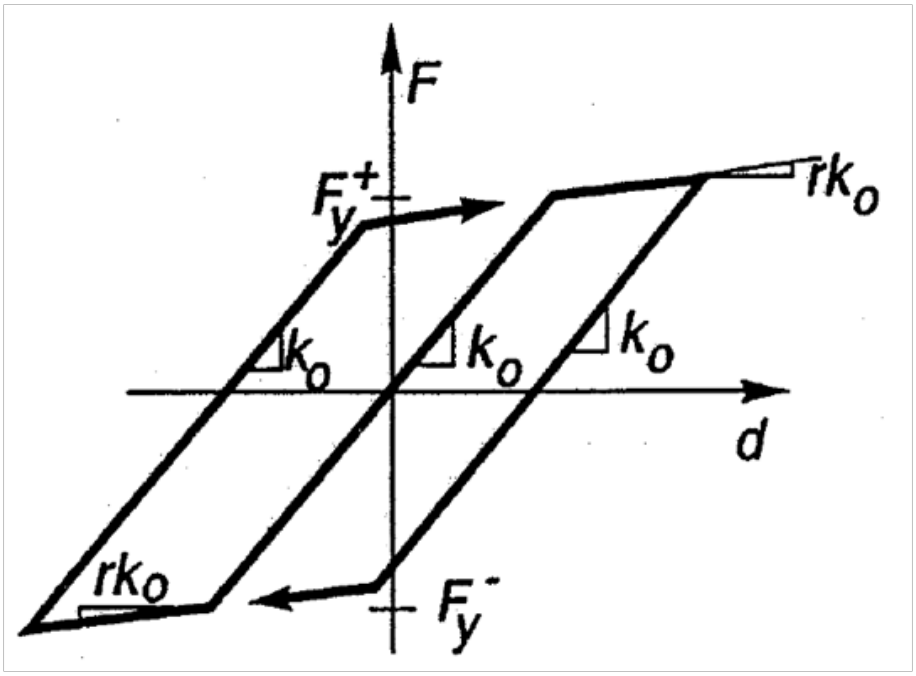

Figure 3.3 Bi-linear hysteretic model used to model BRBs. (Carr 2002)

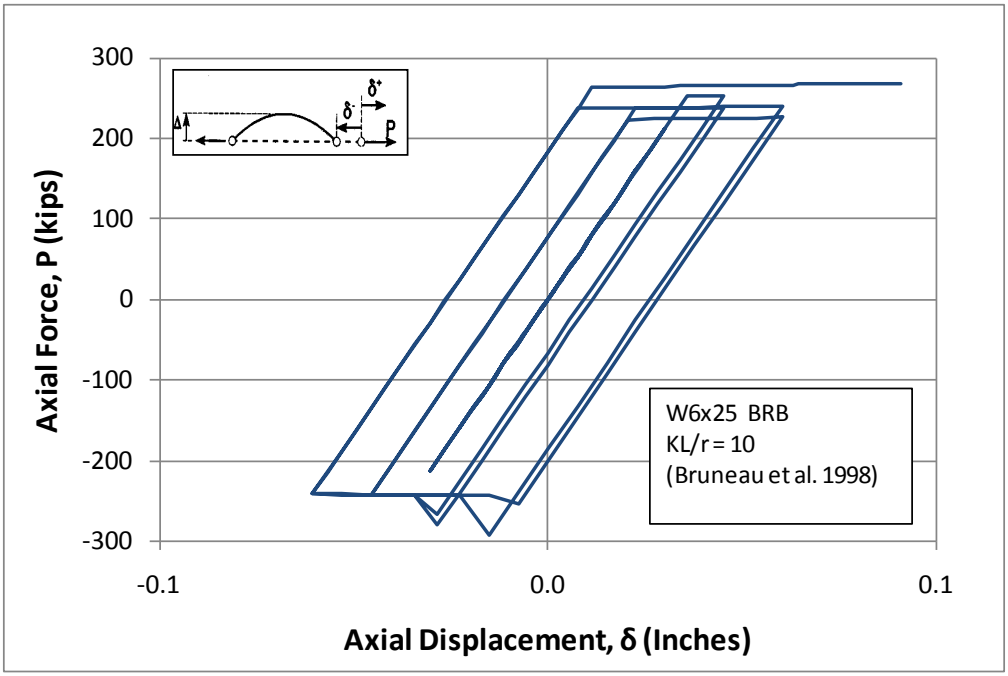

Figure 3.4 HYSTERES-modeled BRB hysteretic brace behaviors modeled using bi-linear model.

4.0 BRACED FRAME ANALYSIS

Having established an understanding of the Remennikov-Walpole (R-W) brace hysteretic behavior, this chapter presents a series of analyses integrating slender, intermediate, stocky and BRB brace behavior into a prototype braced frame model. All modeling was carried out using the two-dimensional version of RUAUMOKO (Carr 2002). The objective of this study is to assess the potential design space of PBRBs. A series of analyses of a six story CBFs is conducted each incorporating slender, intermediate, stocky and BRB brace behavior. The fundamental question addressed is: *When retrofitting a braced frame, is it always necessary to improve brace behavior to that of a BRB or, under some performance objectives is it adequate to provide something less: a PBRB?* Similarly: *Are BRBs necessary in regions of low or moderate seismicity? Are there applications where a slender, intermediate, or stocky brace will achieve the desired performance objectives?* As such, one may consider the model having the slender brace as being the original building and the intermediate, stocky and BRB braces as being the spectra of possible retrofit measures for the braces. Each model is subject to both nonlinear pushover and nonlinear time history analyses (NLTH) to investigate both global behavior of the building and the local behavior of the braces.

4.1 PROTOTYPE BUILDING

The prototype building used in this study is a six-story split level X-braced frame shown in Figure 4.1. The prototype was designed by Sabelli (2001) in support of his study of BRB behavior. The building has a 13-foot typical story height and 18 foot first story. The prototype plan dimensions are 154 feet square incorporating five 30 foot square bays in both directions and a 2 foot cantilever all around. Six braced bays provide 100% of the lateral force resistance in each direction. The braced bays are located at the exterior of the structure as shown in Figure 4.1. The remaining 'non-frame' columns carry only gravity load. Both frame and non-frame columns change sections and are spliced at the mid-height at the fourth story. The six story frame from Sabelli was selected because it captures the effects of the brace prototypes as they vary over the height of the structure better than a low-rise building. Additionally, the six story structure introduces some degree of higher order mode effects in the dynamic analyses. Taller prototypes were not considered since these are wall-frame structures which complicates the modeling and results in smaller demands on the braced frame portion of the lateral load resisting system. Principle member properties of the prototype braced frame are given in Table 4-1.

Only one braced frame is modeled. Lateral loads are assumed to be carried by the six braces present in each direction equally. Brace columns are modeled as fixed base and carry only their tributary gravity loads (Appendix A). To model the inertial effects of building mass, a 'dummy' column having lateral degrees of freedom constrained to those of the braced frame is modeled. The 'dummy' column not only allows the appropriate vertical distribution of mass but also accounts for the small lateral stiffness associated with the gravity load carrying columns (see Table 4-1). Thus, the dummy column has a moment of inertia and moment capacity equal to the sum of the corresponding values for all of the columns in the gravity-only frames divided by the

number of braced frames oriented in the direction of the ground motion (six). Model geometry, including node and member numbering is shown in Figure 4.2.

In RUAUMOKO (Carr 2002), braces were modeled using one-component (Giberson) beam elements with their rotational degrees of freedom released so that the member carries only axial load. Sample calculations of brace capacity are presented in Appendix B. Standard beam-column elements were used to model all beams and columns. Sample calculations for determining the beam-column axial load-moment interaction functions are presented in Appendix C. Typical Rayleigh damping of 5% for steel braced frames was considered in the analysis.

4.2 PROTOTYPE FRAME BRACES

The prototype braces (Table 4-1) considered in the analysis were selected based on the analyses conducted by Sabelli (2001). In RUAUMOKO, the braces were modeled using the R-W hysteresis rule. Sample brace input parameters (for the 1st floor brace – element 34) are given in Table 4-2 and described in Chapter 3. In order to model the varying slenderness while continuing to use the same brace section and length, the effective length factor (k) was modified to affect the desired slender (kL/r = 120), intermediate (kL/r = 80) or stocky (kL/r = 40) behavior. The modification was made as follows:

The HSS 10x10x1/2 brace member has a radius of gyration, r = 3.84 in. The ground floor brace length is 281 in. In order to achieve the desired slender behavior, kL/r is set to 120 and the appropriate value of k is determined: kL/r = 120 = k(281)/3.84 $\rightarrow$ k = 1.64. While artificial, this calibration is numerically correct and results in the desired brace behavior and allows the spectra

of brace behavior to be investigated without changing other parameters critical to the overall frame behavior.

The buckling restrained brace was modeled in RUAUMOKO using the bi-linear hysteresis shown in Figure 3.3 with the biaxial factor r = 0.2. All braces are HSS members, therefore F_Y is taken as 46 ksi in all analyses.

4.3 DESCRIPTION OF LOADING

Two analyses were conducted: a) a nonlinear time history (NLTH) analysis using the 1940 El Centro NS ground motion record; and b) an adaptive pushover analysis. The following sections describe the loading used in these analyses.

4.3.1 Gravity Loads

Since only seismic loads are considered in the analyses, only the seismic weight is required. For a structure having no significant storage or snow loads (both are assumed), the seismic weight is equal to the structural dead load. Load take-offs are presented in Appendix A. gravity loads tributary to each frame column are included in all analyses. Seismic mass tributary to each braced frame (one sixth of the total) is applied to the dummy column so as only to affect the correct dynamic properties of the model without affecting the behavior of the braced frame.

4.3.2 Non-Linear Time History

A non-linear time history (NLTH) analysis applying the 1940 El Centro NS ground motion to each frame model was conducted using RUAUMOKO. The ground acceleration was scaled by a factor of two to obtain significant non-linear behavior in the frame. The twenty second ground motion record is digitized at 0.02 seconds. The time step applied in the analysis was 0.005 seconds. The ground motion record and its acceleration response spectra (5% damping) are shown in Figure 4.3. The El Centro record was selected due to its broad spectral response across all periods less than 1 second (Figure 4.3b). The first six mode periods and mass participation are reported in Table 4-3. Vertical excitation (modes 3 and 6) was neglected in this two dimensional NLTH analysis. Therefore, no mass (and thus no mass participation) was assigned in the vertical direction.

A non-linear time history is performed using direct integration numerical methods. NLTH problems are solved using numerical time-stepping methods for integration of the differential equations of motion:

$$[M]\{X''\} + [C]\{X'\} + [K]\{X\} = F(t) \qquad (Eq.\ 4.1)$$

Where F(t) is the dynamic forcing function, M is the structure mass, C the damping, K the stiffness, and X is the resulting displacement as a function of time X(t). X' is the system velocity and X" is the system acceleration. The numerical solution of Eqn 4-1 gives the displacement response of the structure, and the internal forces can be determined from the displacements. In RUAUMOKO, a 0.005 time step, four times greater than the time step of the

forcing function, F(t), was selected and the Newmark implicit method of integration was used to solve the equations of motion.

4.3.3 Pushover Loading

Nonlinear pushover analysis (often referred to as nonlinear static analysis or NLSA) is a relatively simple solution to the complex problems of predicting force and deformation demands imposed on a structure by severe ground motions. NLSA is common in practice since a) it is simple; b) it does not require the dynamic properties of the structure to be known or calculated; and c) it eliminates the uncertainty involved in selecting appropriate ground motions for a NLTH analysis. Using a RUAUMOKO, a pushover analysis is easily achieved using a slow ramp function as the dynamic force excitation (rather than a ground motion). The ramp duration must be sufficiently long to not impart inertial effects in the model. Typically, the ramp duration must be at least ten times the fundamental period. In the analyses conducted here, the ramp used was 10 seconds long.

RUAUMOKO permits an ‘adaptive pushover’ analysis to be conducted. An adaptive pushover analysis changes the loading pattern to reflect the deformation pattern of the structure. An initial loading pattern is defined and used for the first step of this analysis. For this analysis, the initial pattern used was the inverted triangular pattern used in a conventional pushover analysis. Carr (2002) states that the adaptive pushover behavior shows little sensitivity to selection of the initial load pattern. As the load is increased, the loading pattern adapts to the deformations of the structure to more accurately represent the true inertial load distribution along

the height of the structure (Carr, 2002). Thus the adaptive pushover captures some of the effects of higher modes.

4.4 TIME HISTORY RESULTS AND DISCUSSION

Table 4-4 summarizes key response parameters obtained from the NLTH analyses including peak roof displacement, interstory drift and energy dissipated during the scaled 20 second El Centro event.

The relatively stiff nature of CBF systems is evident in the overall roof drift values which vary from 0.9% to 0.5% as the braces are varied from slender to stocky and BRB. The slender brace model exhibits relatively soft first story behavior, exhibiting a peak interstory drift of 2.2% The soft story behavior is less pronounced as the braces are made progressively more stocky. Typical interstory and roof drift limits for seismic effects are 2%. For the single NLTH conducted, the slender brace model exceeds this limit although it is pointed out that a) the ground motion has been scaled by a factor of 2 for all analyses; and b) the El Centro ground motion is particularly critical for structures having a period under 1 second (Figure 4.3b).

Figure 4.4 shows the displacement time histories of the roof, 4^{th} and 2^{nd} storeys. These histories illustrate the progressively improved response as the braces range from slender to stocky. The dominance of the taller first story drifts in each analysis is evident as the overall displacements are clearly dominated by those resulting from lower in the structure (2^{nd} floor, node 8). The improvement in the degree of nonlinearity in progressively stocky models is also evident as the residual displacement at 20 seconds decreases. It is noted that the El Centro record

is known to result in residual deflections due to a few large pulses early in the record (Figure 4.3a) that tend to push the structure in the same direction.

Figure 4.5 shows the hysteretic behavior of the left-hand brace at the ground floor (element 34 in Figure 4.2). Significant nonlinearity is observed in all models for this critical element. The progressively stiffer behavior of the braces as they vary from slender to stocky and BRB is clearly evident as the brace axial deformations are reduced. All behaviors are similar to those described in Chapter 3 and thus confidence in the models and the use of the R-W hysteretic model is established.

Figure 4.6 shows the drift envelopes for the NLTH analyses. The progressive improvement in behavior as the braces vary from slender to stocky is clearly evident. The shape of these envelopes also indicate the presence of higher mode effects which appear more pronounced in the more flexible (due to greater amount of plasticity) slender model.

Cumulative energy dissipation curves generated from each NLTH analysis are presented in Figure 4.7. The final values of dissipated energy following the 20 second analyses are given in Table 4-4. As expected, the stockier brace models dissipate greater amounts of energy and the proportion of energy dissipated by strain energy increases as the hysteretic behavior improves. For the models studies, the BRB braces saw little inelasticity above the first story in which case the strain energy dissipated was proportionally lower although the total energy dissipated was quite high.

4.5 PUSHOVER RESULTS

Adaptive pushover curves capturing the base shear vs. roof displacement of each model are shown in Figure 4.8.The same trends in behavior as observed in the NLTH analyses are observed here. With progressively stockier braces, the frame capacity increases while its displacement capacity falls. While only the slender brace model is able to achieve the 2% roof drift limit prescribed by ASCE 7 (2008), this is not a great concern since CBF systems are quite stiff and will rarely see drifts exceeding 1% in practice. As appropriate for a envisioning the progression of brace slenderness as being surrogate for brace retrofit, the structure stiffness is not affected by changes in the brace behavior.

4.6 COMPARISON OF MODELS

Table 4-5 provides key performance parameters normalized to those obtained for the slender brace model. Thus the normalized drifts are less than 1.0 and the normalized energy dissipation is greater than 1.0.

It is understood that this modeling exercise is artificial and that inferences about the frame design are inappropriate. Nonetheless, the comparison of model response parameters and the trends identified are valid and informative. The most striking conclusion of this study is that the relative effect on structural performance by reducing the slenderness of the braces is had as the brace is changed from slender (kL/r = 120) to intermediate (kL/r = 80). The incremental effect of improving the behavior to stocky (kL/r = 40) and eventually to a BRB brace is reduced.

This result is encouraging for the use of PBRBs as a retrofit measure for slender braces. The greatest increment in performance is achieved with the least degree of improvement.

Table 4-1 Prototype braced frame sections.

Story	Brace HSS	Braced Frame Columns	Braced Frame Beams	Non-braced frame columns				
				Interior	Mech.	Perp. BF	ΣI_y (in^4)	ΣZ_y (in^3)
6	5x5x1/2	W14x132	W18x46	W14x43	W14x53	W14x132	862	201
5	6x6x1/2		W14x48					
4	8x8x1/2		W18x46					
3	8x8x1/2	W14x211	W14x48	W14x90	W14x99	W14x211	2376	473
2	8x8x1/2		W18x46					
1	10x10x1/2		W14x46					

Table 4-2 RUAUMOKO brace input parameters
Only first floor brace parameters are shown-member 34 in Figure 4.2

RUAUMOKO input parameter	description (Carr 2002)	Slender Brace	Intermediate Brace	Stocky Brace
I_{minor} (in^4)	minor axis moment of inertia	256	256	256
S_{minor} (in^3)	minor axis plastic section modulus	51.2	51.2	51.2
k	effective length factor	1.64	1.1	0.6
α	strain hardening factor	1.0	1.0	1.0
β	'beta' factor	1.2	1.3	1.4
θ_0	initial out of straightness	0.0	0.0	0.0
E1	effective modulus	1.0	1.0	1.0
E2	effective modulus	1.0	1.0	1.0
E3	effective modulus	1.0	1.0	1.0
E4	effective modulus	1.6	1.6	1.6
N	strain hardening rule selection	0	0	0
SHAPE	cross section type	3	3	3

Table 4-3 Mode shape characteristic for the prototype frame.

Mode	Period (s)	Mass participation (%)
1st mode	0.72	80
2nd mode	0.24	15
3rd mode	0.16	0
4th mode	0.14	4
5th mode	0.12	1
6th mode	0.01	0

Table 4-4 Summary of key results of NLTH analysis

parameter	units	Analysis			
		Slender	Intermediate	Stocky	BRB
Maximum roof displacement (node 27)	in	9.45	5.90	5.23	5.17
… as ratio of building height		0.009	0.006	0.005	0.005
…at time	sec.	3.15	5.45	1.95	1.95
Maximum interstory drift	in	4.76	2.12	1.31	1.24
… as ratio of story height		0.022	0.010	0.006	0.006
… at floor		1	1	1	1
… at time	sec.	3.15	5.45	5.40	5.30
Total kinetic energy dissipated	kip-in	10,000	6,000	8,000	10,000
Total damping energy dissipated	kip-in	100,000	53,000	98,000	165,000
Strain energy dissipated	kip-in	75,000	151,000	181,000	118,000
Total energy dissipated	kip-in	185,000	210,000	287,000	293,000

Table 4-5 Key results normalized by those for slender analysis

Parameter	Analysis			
	Slender	Intermediate	Stocky	BRB
Maximum roof displacement (node 27)	1.0	0.62	0.55	0.54
Maximum interstory drift	1.0	0.45	0.28	0.26
Total kinetic energy	1.0	0.60	0.80	1.00
Total damping energy	1.0	0.53	0.98	1.65
Strain energy	1.0	2.01	2.41	1.57
Total energy	1.0	1.14	1.55	1.58

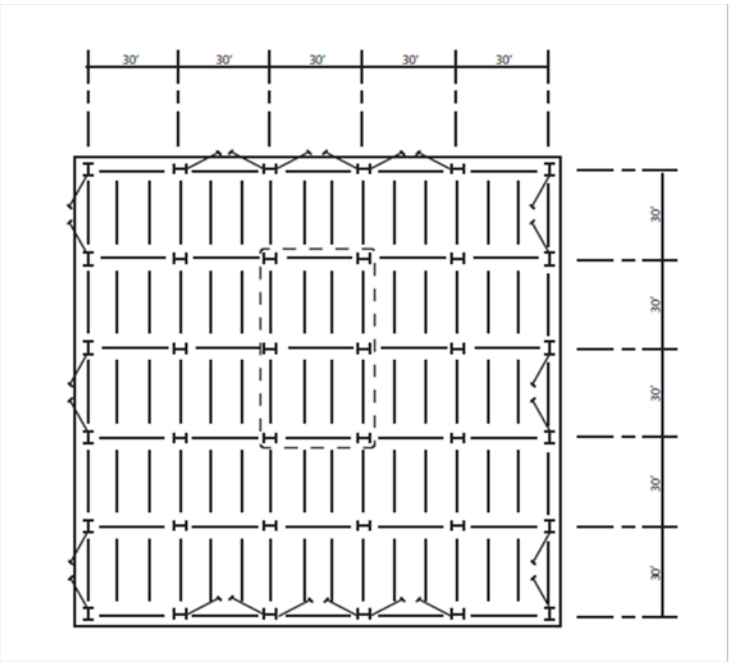

a) Plan (b) Elevation of one brace

Figure 4.1 Prototype Structure. (Sabelli 2001)

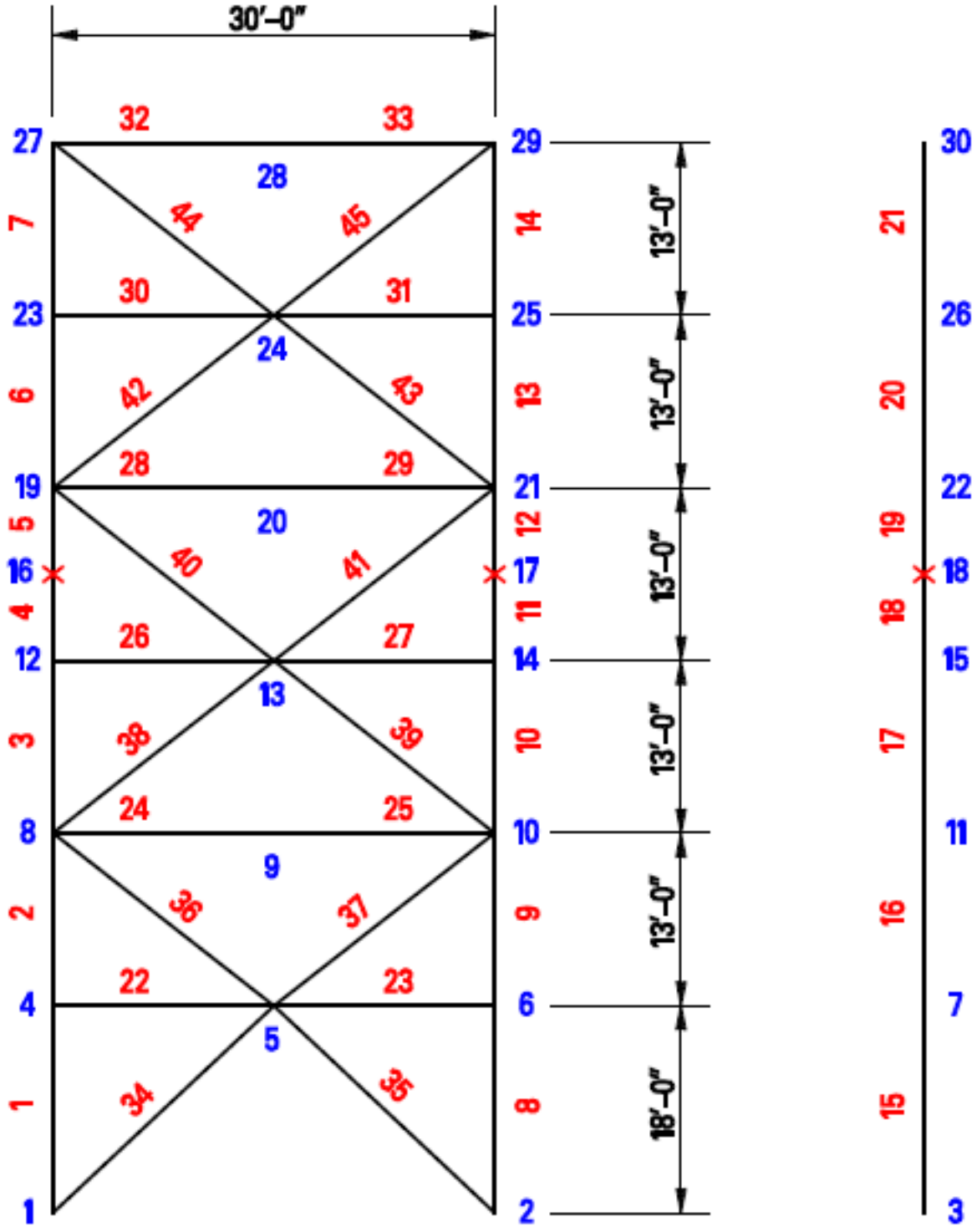

Figure 4.2-Prototype split level x-frame building.

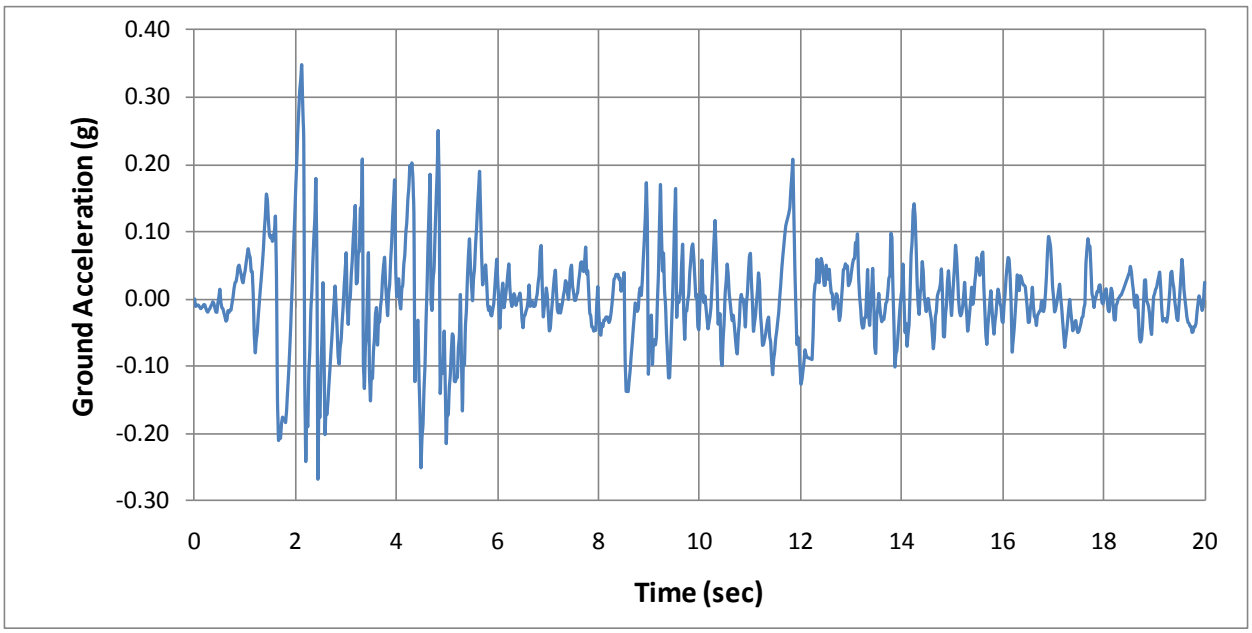

a) unscaled acceleration time history

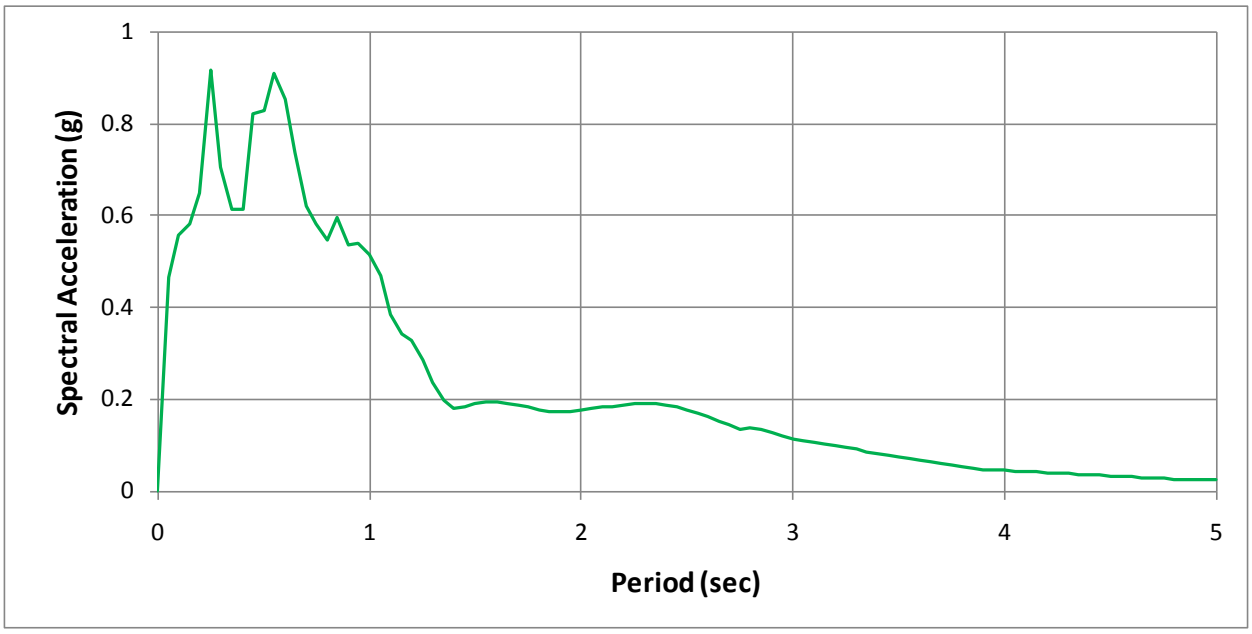

b) 5% damping response spectra

Figure 4.3- 1940 El Centro ground motion used in NLTH

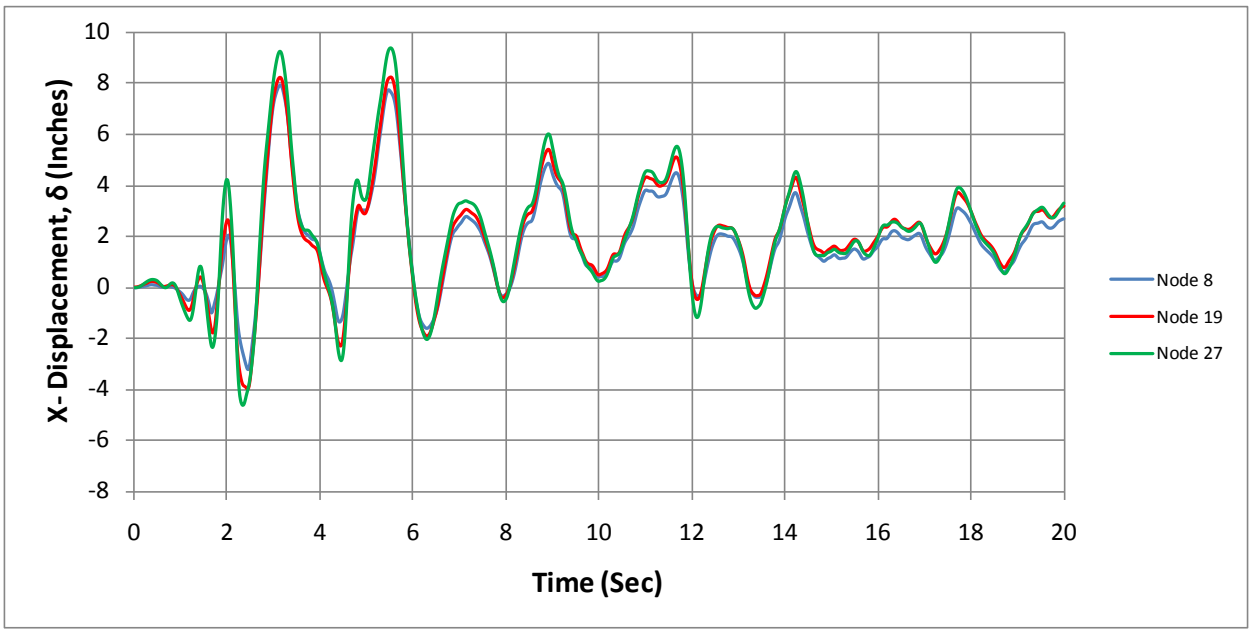

a) representative slender brace NLTH

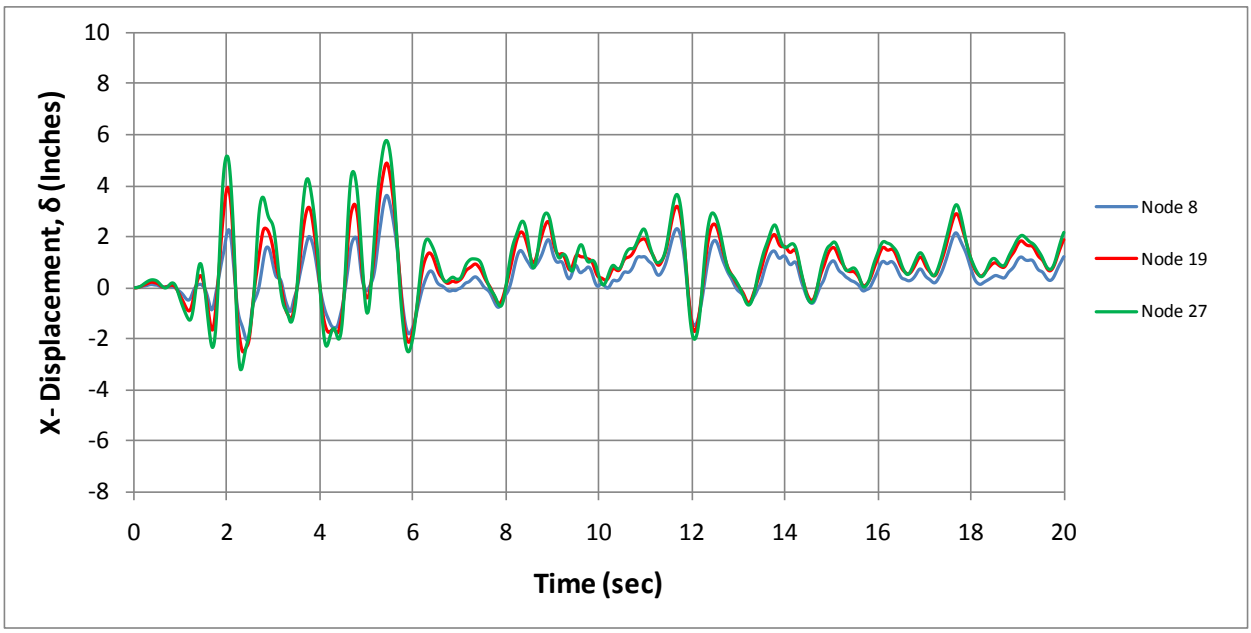

b) representative Intermediate brace NLTH

Figure 4.4- NLTH displacement-time histories

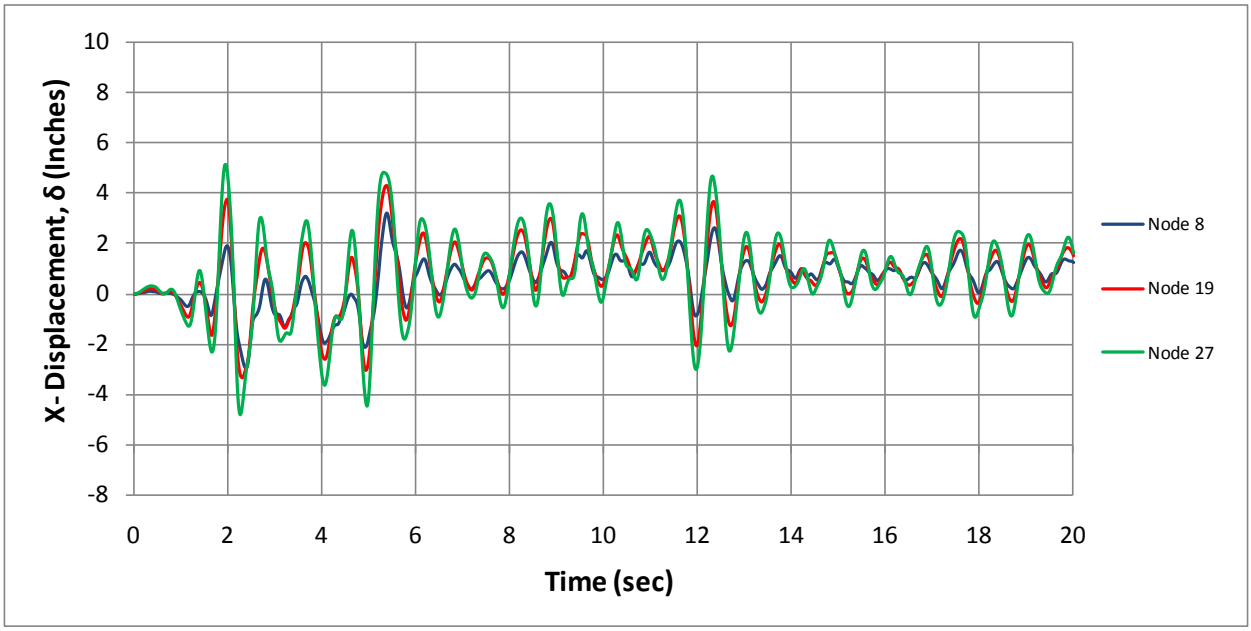

c) representative stocky brace NLTH

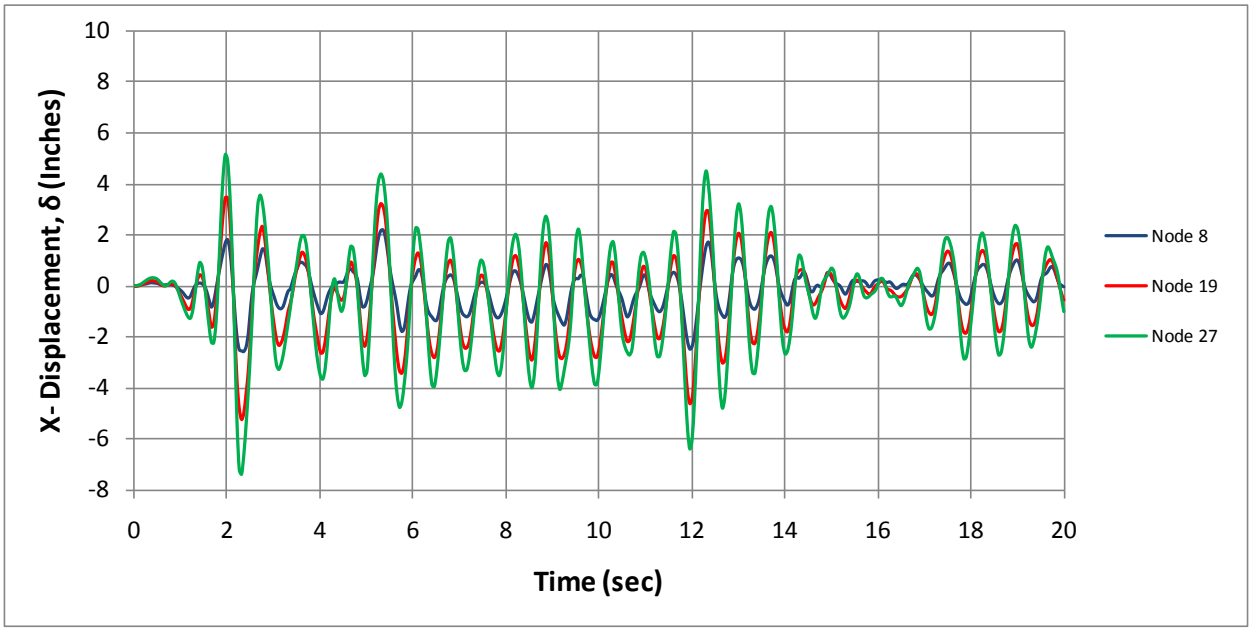

d) representative BRB NLTH

Figure 4.4 (continued) NLTH displacement-time histories

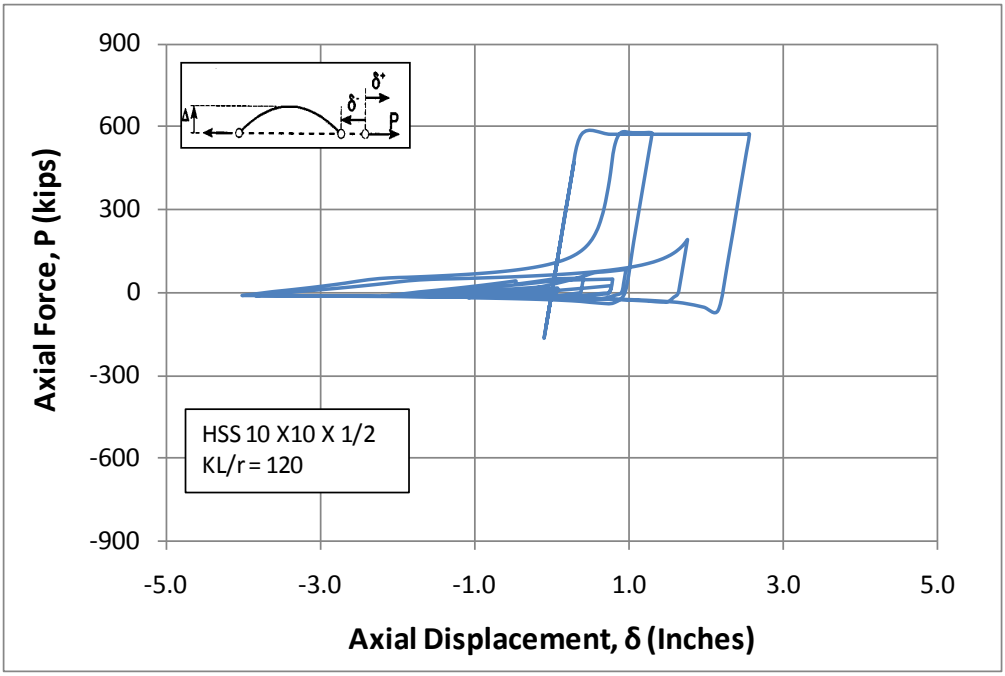

a) representative slender brace hysteresis

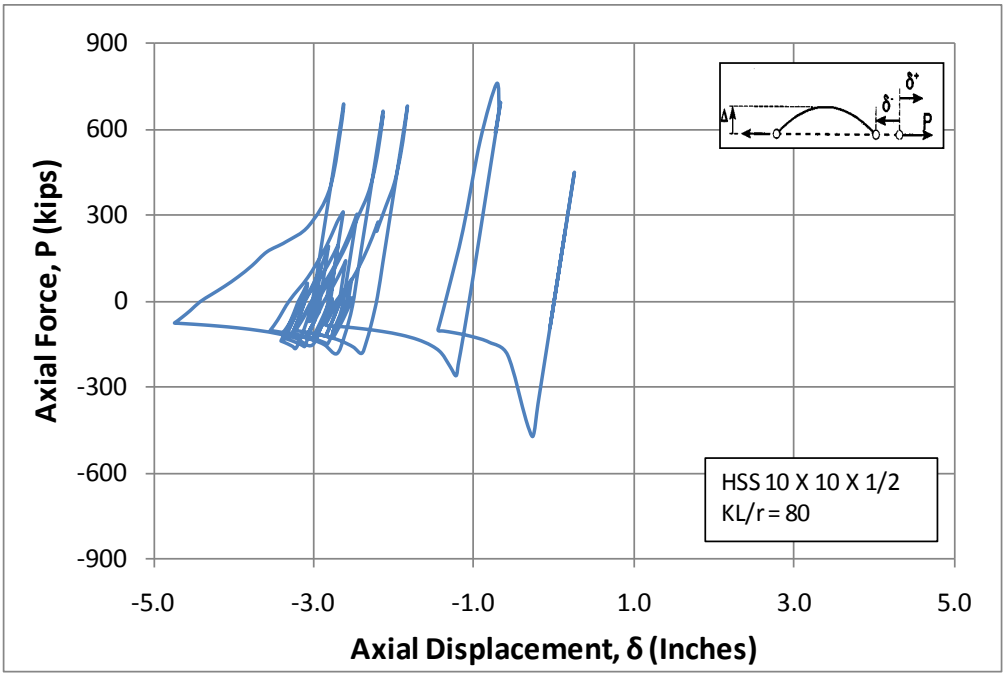

b) representative intermediate hysteresis

Figure 4.5 Brace hysteretic behavior-Element #34

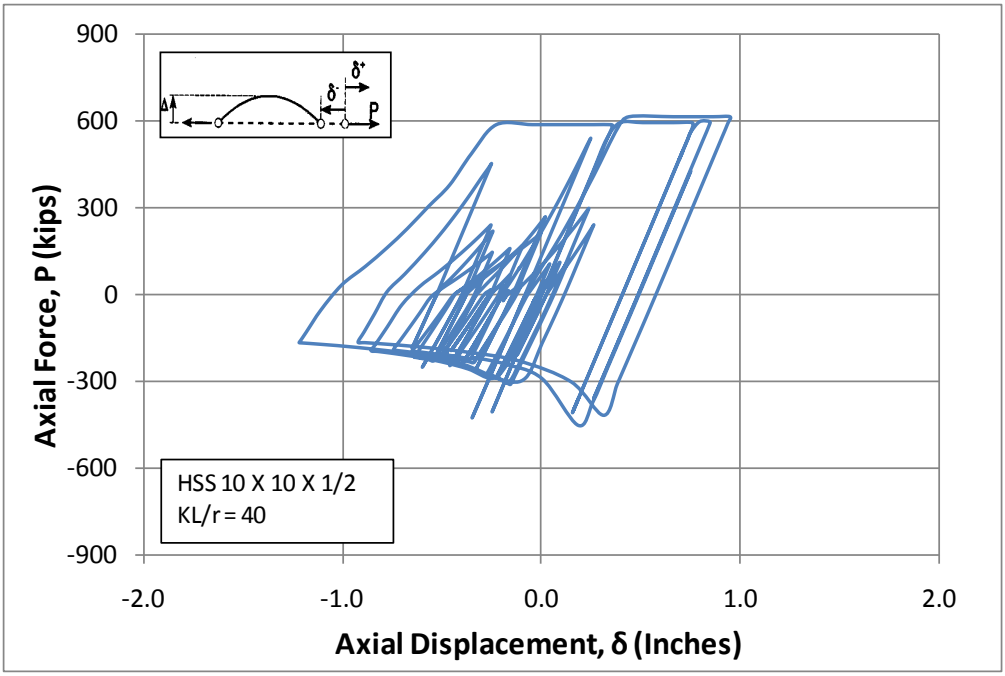

c) representative stocky brace hysteresis

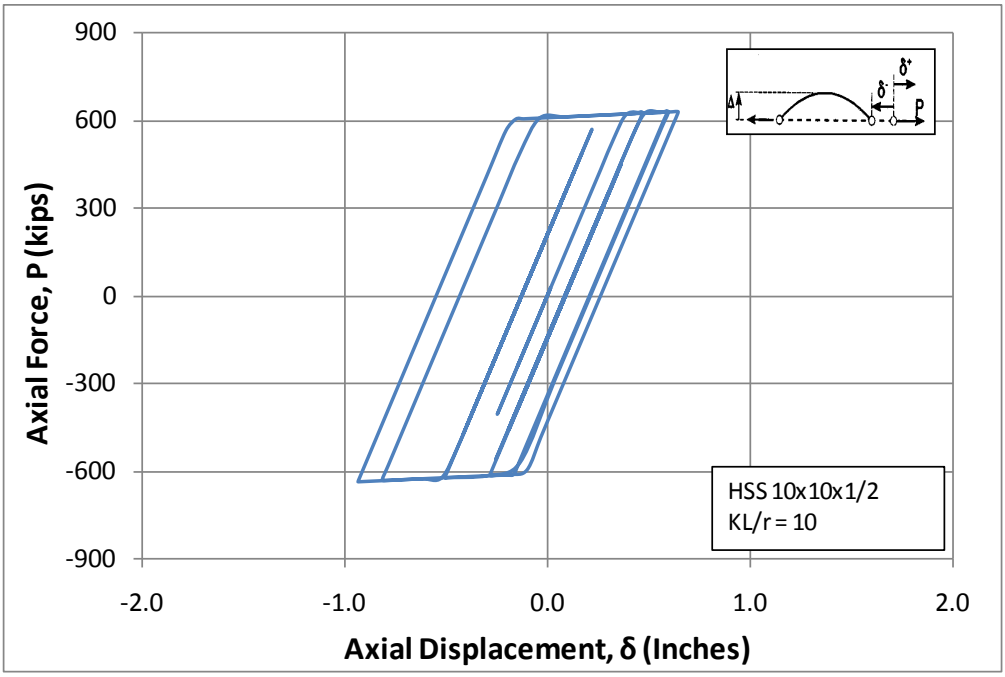

d) representative BRB hysteresis

Figure 4.5 (continued) Brace hysteretic behavior-Element #34

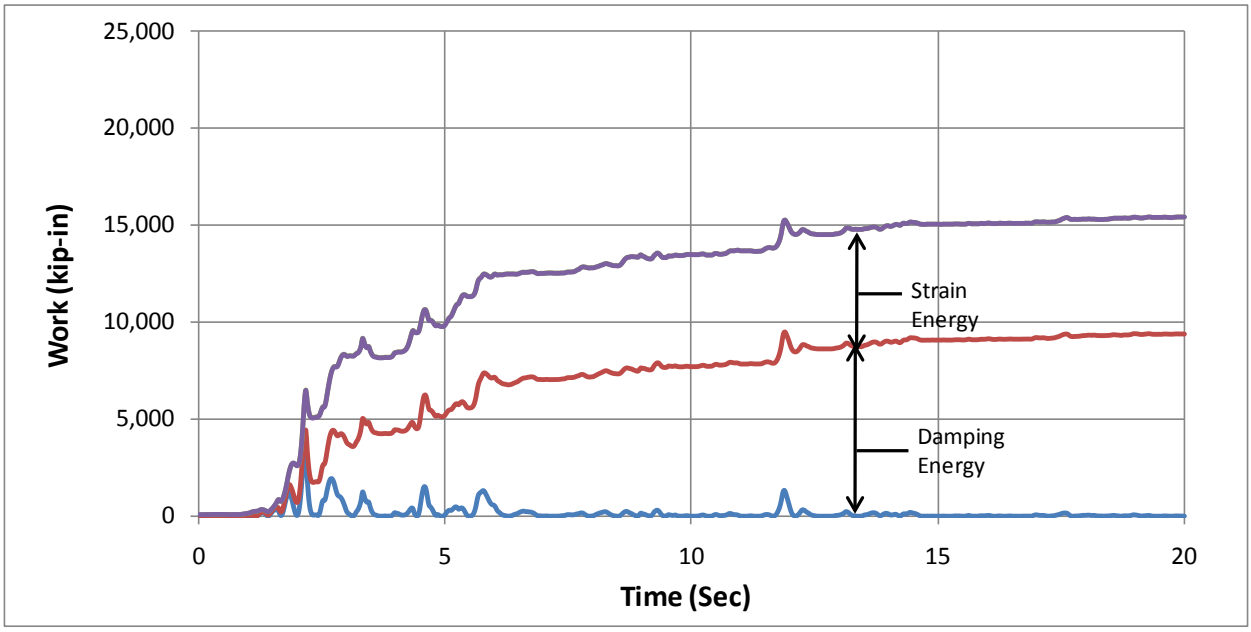

a) representative slender brace energy dissipation

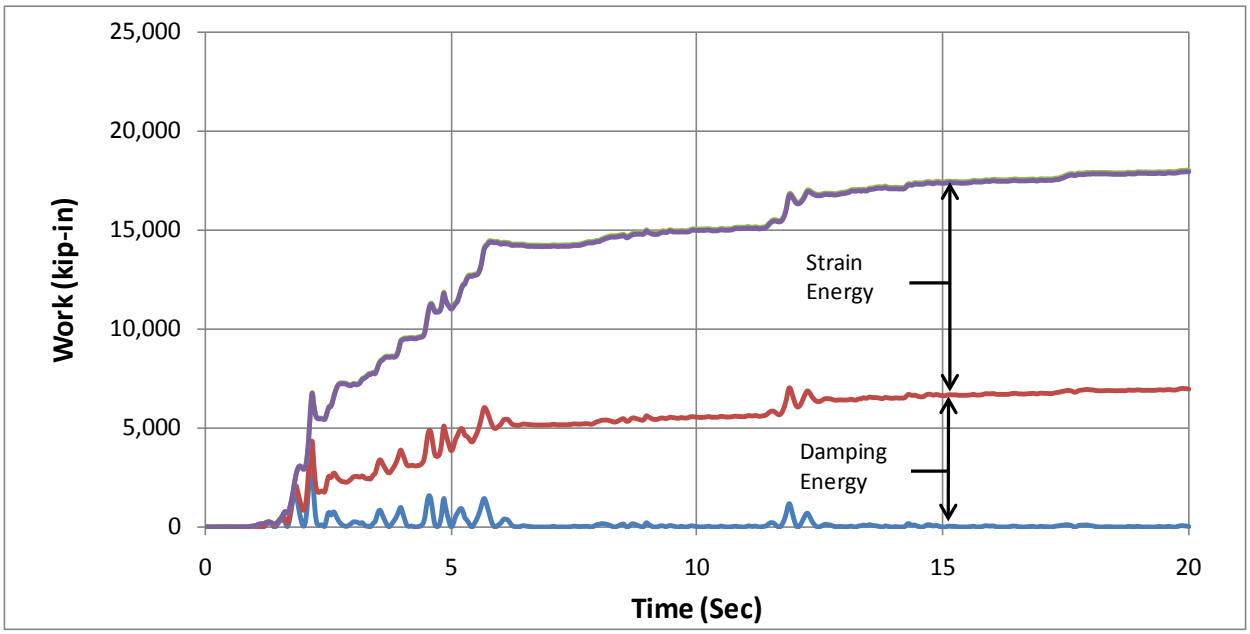

b) representative intermediate energy dissipation

Figure 4.6 Braced Frame Energy Dissipation

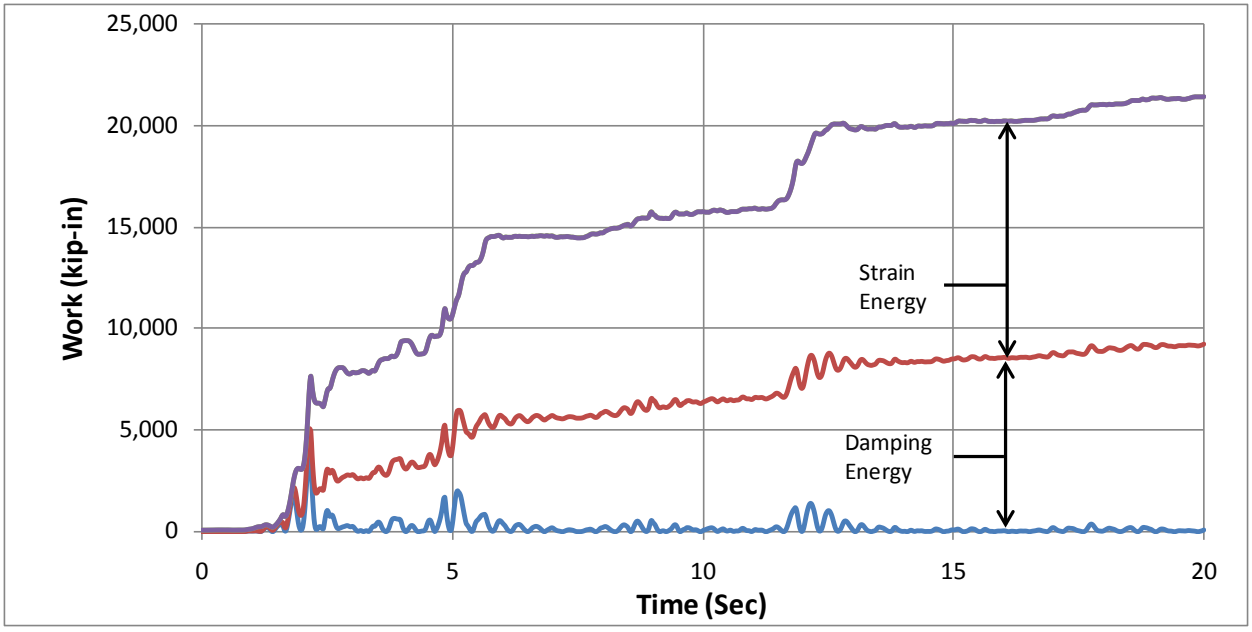

c) representative stocky brace energy dissipation

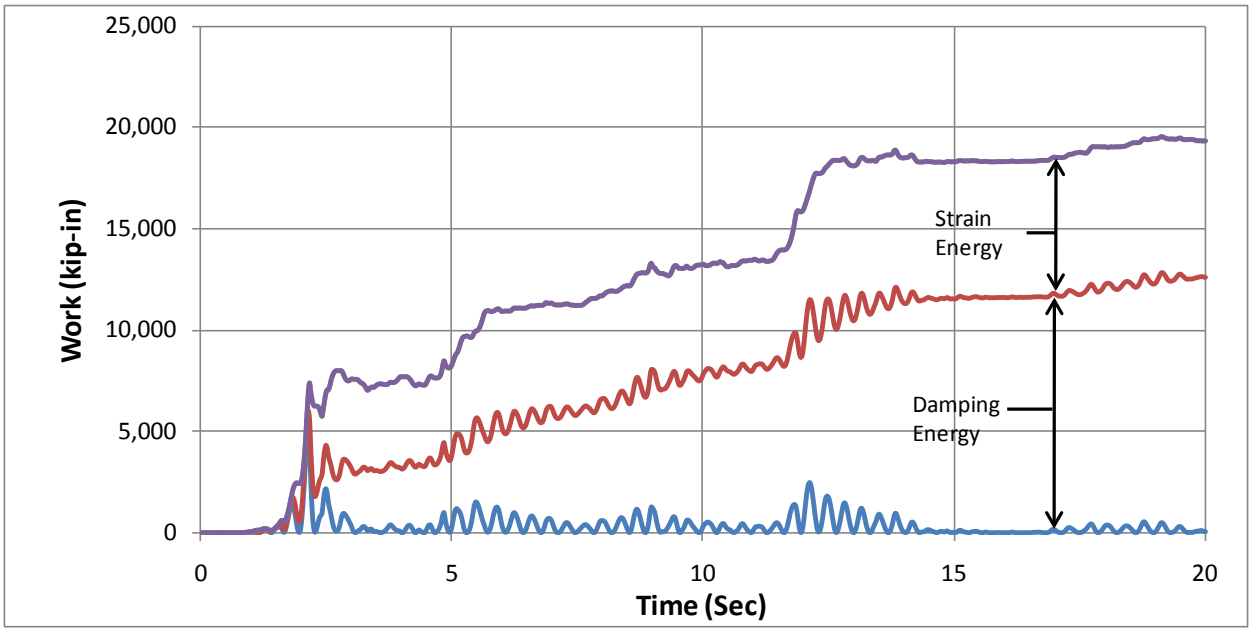

d) representative BRB energy dissipation

Figure 4.6 (continued) Braced Frame Energy Dissipation

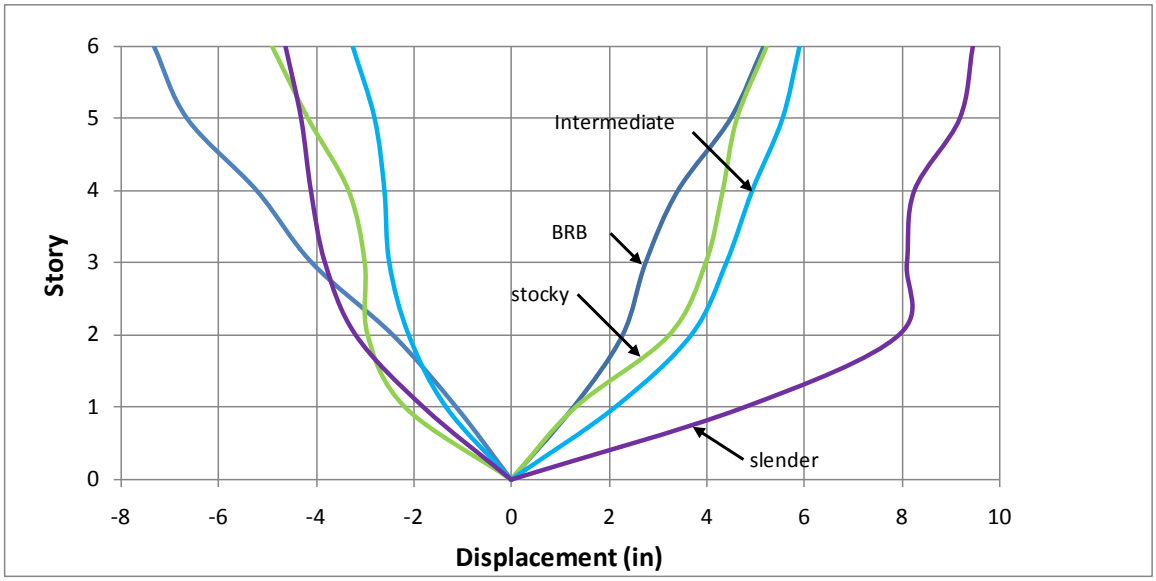

Figure 4.7 Maximum Displacement Envelopes

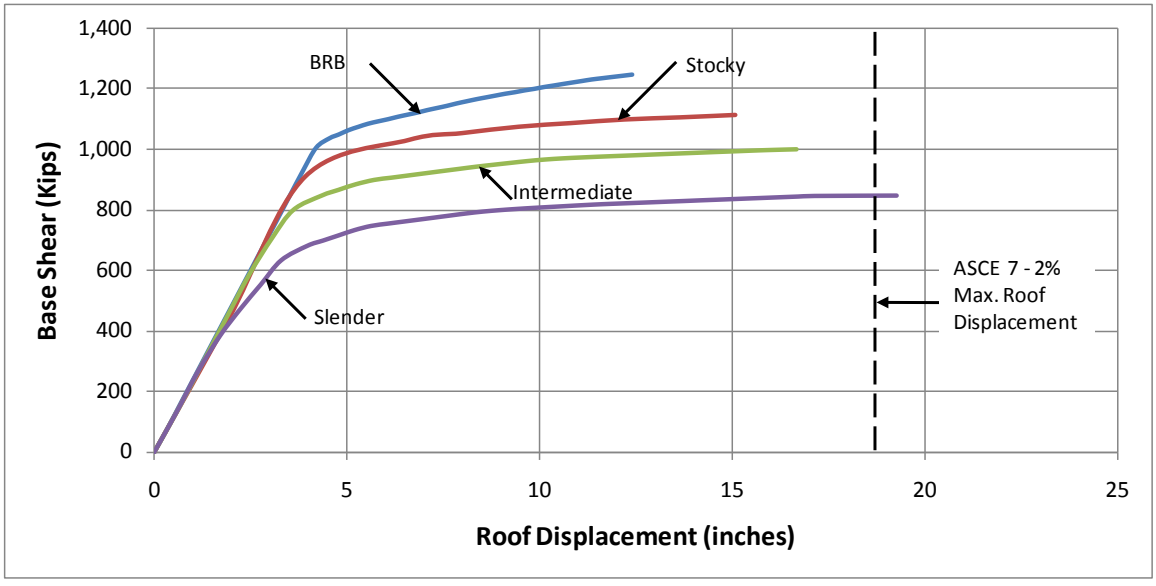

Figure 4.8 Adaptive Pushover Curves

5.0 CONCLUSIONS

The objective of this thesis was to evaluate the potential design space or viability of partially buckling restrained braced (PBRB) elements. These PBRB are envisioned as retrofit measures for slender braces in moderate seismic zones (Harries et al. 2009). PBRBs are a reduced performance alternative to buckling restrained braces (BRB) which are often cumbersome and may be over-engineered for some applications.

A spectra of brace behaviors, ranging from ‘slender’, through ‘intermediate’ and ‘stocky’, to a BRB was presented. Individual brace behavior was investigated and validated against experimental data in Chapter 3. Nonlinear time history (NLTH) and pushover analyses of a six story braced frame provided with the spectra of brace behavior were presented in Chapter 4. The latter portion of this study was intended to address the following two questions:

What is the the potential for the use of PRBBs in retrofitted structures?

The spectra of brace behavior demonstrated in the NLTH analyses illustrates that the potential use of a PBRB system is viable. The structural behavior improved as the braces progressed from slender to stocky to BRB. The incremental improvement is most significant as one improves upon slender behavior and becomes less pronounced as the brace slenderness is reduced. This result is encouraging for the use of PBRBs as a retrofit measure for slender braces. The greatest increment in performance is achieved with the least degree of improvement.

Is it necessary to used BRBs in low to moderate seismic region? Can a reduced performance brace be used?

While BRB performance is superior, the present analyses demonstrate that very good performance can be achieved with non-slender conventional braces. While only a single structure was considered, the trends relating structural and brace performance described in Chapter 4 suggest that BRBs may not be required to achieve adequate structural performance, particularly in less-than-severe seismic zones. Again, this conclusion points to the promise for retrofitting existing slender braces rather than replacing them altogether.

Specific conclusions and outcomes of the present study are as follows:

1. A fundamental understanding of the Remennikov-Walpole (R-W) brace buckling hysteretic model has been established. This model has been validated against experimental brace behavior found in the literature.
2. Braced frame behavior, as measured by displacement, interstory drift or energy dissipation, can be improved upon significantly by reducing the slenderness of the braces.
3. Improvement in structural behavior is incrementally more pronounced at higher brace slenderness ratios; i.e.: changing behavior from slender to intermediate has a greater impact on structural performance than changing from intermediate to stocky.
4. Using a pushover analysis, it is shown that with progressively stockier braces, the frame capacity increases while its displacement capacity falls. While only the slender brace model was able to achieve a 2% roof drift limit, this is not a great concern since CBF systems are quite stiff and will rarely see drifts exceeding 1%.
5. As appropriate for a envisioning the progression of brace slenderness as being surrogate for brace retrofit, the structure stiffness is not affected by changes in the brace behavior.

Having established the viability of PBRB behavior from a structural perspective, additional experimental and analytical research should be initiated to explore this nascent type of FRP-repaired brace and establish the range of parameters and performance improvement that can be achieved. The limited scope of the present study should be expanded upon to encompass a broader range of structural parameters. In accordance with ASCE 7 (2008), a suite of ground motions should be utilized in an extended NLTH program.

APPENDIX A

GRAVITY LOAD CALCULATIONS FOR FRAME ANALYSIS

Gravity loads for seismic analysis were calculated based upon the loading given by Sabelli (2001) shown in Table A-1. It is assumed that the structure has an office occupancy and is located in a region having no appreciable snow loads; therefore the seismic weight, W, is equal to the structural dead load. A plan of the six story building, having uniform 30 foot square bays, is shown in Figure 4-1. There are 12 identical frames, six in each principle direction, located around the building perimeter. Each frame is therefore assumed to resist inertial forces associated with 1/6 of the storey mass. These masses are applied to the 'dummy' column in the analysis (Figure 4-2) and contribute only to the calculation of the dynamic properties of the structure. The resulting floor area tributary to each frame is:

(1/6)(154 x 154) = **3953 square feet**

Similarly, the curtain wall weight tributary to each frame is:

(1/6)(158 x 4) = **103 linear feet/floor** (on average)

In addition, the actual weight carried by each column of the frame must be determined and included in the analysis. The floor area tributary to each frame column is:

30 x 15 = **450 square feet**

The curtain wall weight carried by each frame column is: **30 linear feet/floor**

Table A-1- Gravity load values. (Sabelli 2001)

	Occupied floors	**Roof**	**Mechanical penthouse**
Total Area	23716 sf	21916 sf	1800 sf
Steel framing (assumed)	5 psf	5 psf	5 psf
Floor system (3" deck with 2.5" NWC)	51 psf	51 psf	51 psf
Roofing	-	7 psf	7 psf
Ceilings/Floors	3 psf	-	-
Mechanical/electrical	7 psf	7 psf	47 psf
Partitions	10 psf	-	-
Total real weight	**76 psf**	**70 psf**	**110 psf**
Exterior wall (25 psf)	325 plf (13 feet)	88 plf (42" parapet)	-

Thus the values used for gravity loads and masses in the frame analysis are as follows:

Table A-2- Resulting loads and masses assigned to braced frame model.

	Nodes in Model (Figure 4-2)	**Occupied floors**	**Roof**
story mass	7,11,15,22,26,30	3952 sf x 76 psf = 300.3 kips	288.6 kips
curtain wall		106 lf x 325 plf = 34.4 kips	9.4 kips
Total Story Mass		**334.7 kips**	**298.0 kips**
load on frame column	4,8,12,19,23,27,6,10,14,21,25,29	450 sf x 76 psf = 34.2 kips	31.5 kips
curtain wall		30 lf x 325 plf = 9.8 kips	2.6 kips
Total Column Load		**44.0 kips**	**34.1 kips**

APPENDIX B

EXAMPLE CALCULATIONS OF BRACE AXIAL TENSION AND COMPRESSION CAPACITIES

SLENDER BRACE ($\frac{KL}{r} = 120$):

Brace shape: HSS 10x10x1/2

A_g = 17.0 in^2	E = 29000 ksi	F_Y = 46 ksi
r = 3.86 in	L = 281 in	k = 1.65

Axial Tension Capacity $T_{CAP} = A_g F_Y = 782\ kips$ AISC Eq. E3-4

Axial Compression Capacity= $C_{CAP} = A_g F_{cr} = 296\ kips$

Where $F_{cr} = \left(0.658^{\frac{F_Y}{F_E}}\right) F_Y = 17.4\ ksi$ AISC Eq. E3-2

$F_E \frac{\pi E}{\left(\frac{kL}{r}\right)^2} = 19.8\ ksi$ AISC Eq. E3-4

Note that inelastic buckling (AISC EQ E3-2) is assumed for all cases although the limiting slenderness for using this equation is $\frac{kL}{r} < 4.71\sqrt{\frac{E}{F_Y}} = 118$.

APPENDIX C

EXAMPLE CALCULATION OF BEAM-COLUMN YIELD INTERACTION SURFACE

For beam column elements, an axial load-moment interaction behavior is required. RUAUMOKO utilizes an interaction surface shown in Figure C-1. The values at the control points are defined as follows:

Element 1 –W14x211

E = 29000 ksi F_y = 50 ksi

k_x = 0.65 L = 156 in r_x = 6.55 in I_x = 2660 in^4 A= 62 in^2

k_y = 0.65 r_y = 4.07 in I_y = 1030 in^4

$\frac{kL}{r_x} = 15.5$ $\frac{kL}{r_y} = 24.9$ k_y controls

PYC = Axial Compression Yield Force

$\lambda_c = \frac{\frac{k_y L}{r_y}}{\pi\sqrt{\frac{E}{F_Y}}} = 0.329$ λ_c = 0.329 ≤ 1.5, therefore, buckling is inelastic

$F_{cr} = \left(0.658^{\lambda_c}\right)F_Y = 47.7\ ksi$ F_{cr} = 47.7 ksi

PYC = F_{cr}A = **2957 kips**

PYT = Axial Tension Yield Force

PYT = F_yA = **3100 kips**

M0 = Yield Moment at P = 0

$L_{p1} = 1.76 r_y \sqrt{\frac{E}{F_Y}} = 176.1\ in = 14.38\ ft$ L_{p1} > L, therefore, M0 = bM_p

M_p values from AISC (2005) Table 5-3

M0 = M_p = **17520 k-in**

PB = Axial Compression Force at B on the interaction diagram

P_B = 0.2PYC = **591 kips**

MB = Yield Moment at B on the interaction diagram

M_B = 0.9M0 = **15768 k-in**

PC = Axial Compression Force at C on the interaction diagram

P_B = 0.2PYT = **620 kips**

MC = Yield Moment at B on the interaction diagram

M_C = 0.9M0 = **15768 k-in**

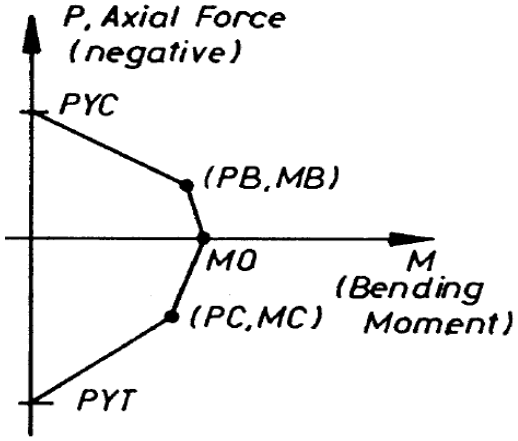

Figure 5.1 RUAUMOKO P-M Interaction surface

BIBLIOGRAPHY

Abraham, E.J, and Harries, K.A. (2006) "Development of "Partial Buckling-Restrained Braces" using FRP" *Proceedings of the ASCE STRUCTURES 07 Congress*, Long Beach CA, May 2007.

American Institute of Steel Construction (AISC). (2005a) *Steel Construction Manual*, 13th Edition.

American Institute of Steel Construction (AISC). (2005b) *ANSI/AISC 341-05 Seismic Provisions for Structural Steel Buildings.*

American Society of Civil Engineers (ASCE), 2008. SEI/ASCE 7- *Minimum Design Loads for Buildings and Other Structures*, American Society of Civil Engineers, Reston VA.

Black, G.R., Wenger. W.A., and Popov, E.P. (1980) " Inelastic Buckling of Steel Struts under Cyclic Load Reversals." Report *No. UCB/EERC-80/40*, Berkeley: Earthquake Engineering Research Center, University of California.

Black, C.J., Makris, N., and Aiken, I.D. (2004) "Component Testing, Seismic Evaluation and Characterization of Buckling-Restrained Braces." *ASCE Journal of Structural Engineering*, Vol. 130, No. 6, pp 880-894.

Bruneau, M., Uang C.M., and Whittaker, A. (1998) *Ductile Design of Steel Structures*. McGraw-Hill, Boston.

Bruneau, M. and Lee, K. (2005) "Energy Dissipation of Compression Members in Concentrically Braced Frames" *ASCE Journal of Structural Engineering*, Vol. 131, No. 4, pp 552-559.

Carr, A. (2000) *RUAUMOKO – Inelastic Dynamic Analysis Computer Program*. University of Canterbury, NZ.

Goel, S.C. (1992) "Earthquake Resistant Design of Ductile Braced Steel Structures," *Stability and Ductility of Steel Structures under Cyclic Loading*, pp 297-308.

Harries, K.A., Peck, A. and Abrahams, E.J. (2009) "Enhancing Stability of Structural Steel Sections using FRP", *Thin Walled Structures*, special issue on FRP Strengthened Metallic Structures Vol. 47, No. 10, pp 1092-1101.

Ikeda, K. and Mahin, S.A. (1986) “Cyclic Response of Steel Braces” *ASCE Journal of Structural Engineering*, Vol. 112, No. 2, pp 342-361

Jain, A. (1978) “ Hysteresis models for steel members subjected to cyclic buckling or cyclic end moments and buckling” University of Michigan, Report No. UMEE78R6, pp. 98.

Khatib, I., and Mahin, S. (1988) “Seismic Behavior of Concentrically Braced Steel Frames”. *Earthquake Engineering Research Center*, January 1988.Remennikov, A. and Walpole, W. (1997) “Analytical Prediction of Seismic Behavior for Concentrically Braced Steel Systems”. *Earthquake Engineering and Structural Dynamics*, Vol. 26, pp 859-874.

Sabelli, R. and Lopez, W. (2004) “Design of Buckling Restrained Braced Frames”, *Modern Steel Construction*, March 2004.

Sabelli, R. (2001) *Research on Improving the Design and Analysis of Earthquake-Resistant Steel Braced Frame.* Earthquake Engineering Research Institute. NEHRP Professional Fellowship in Earthquake Hazard Reduction, October 2001.

Wakabayashi M, Nakamura T., Katagihara A., Yogoyama H., Morisono T. (1973) “Experimental study on the elasto-plastic behavior of braces enclosed by the precast concrete panels under horizontal cyclic loading- Parts 1 & 2.” *Summaries of technical papers of annual meeting.* Vol. 10. Architectural Institute of Japan, Structural Engineering Section, pp 1041-1044 [In Japanese].

Xie. Q. (2005) “State of the art of buckling-restrained braces in Asia.” *Journal of Constructional Steel Research*, Vol. 61, No. 6, pp 727-748.